공학석사 학위논문

Transport of Microplastics in Marian Cove, West Antarctica

서남극 마리안 소만에서의
미세플라스틱 이송

2021 년 8 월

서울대학교 대학원
건설환경공학부
김 보 경

Transport of Microplastics in Marian Cove, West Antarctica

서남극 마리안 소만에서의 미세플라스틱 이송

지도교수 황 진 환

이 논문을 공학석사 학위논문으로 제출함

2021 년 5 월

서울대학교 대학원
건설환경공학부
김 보 경

김보경의 석사 학위논문을 인준함

2021 년 6 월

위 원 장 _____

부위원장 _____

위 원 _____

ABSTRACT

Microplastics with a size of less than 5 mm have been discovered in the Antarctic Ocean known as a pristine sea. The origins of microplastics are largely estimated to be both outside and inside Antarctica. According to the survey, more than half of the scientific research stations residing in Antarctica do not have adequate sewage treatment systems, so it could be speculated that the wastewater has a regional effect on pollution in the Antarctic Ocean. Through the field survey, it was confirmed that microplastics were accumulated in Marian Cove where the King Sejong Station is located, and the concentration of microplastics in the wastewater was about 1000 times higher than that of the surrounding seawater. It is expected to be a major cause of microplastic pollution in seawater around the station.

This study performed numerical modeling to elucidate the movement and accumulation mechanism of microplastics in the bay. When reproducing the flow around the station, the waves affecting the movement of microplastics were considered. The trajectories of the particles were then tracked according to waves, release time, and release location by using the Lagrangian Particle Tracking method that reflects the properties of microplastics. As a result of numerical simulation, the flow velocity of Marian Cove is slower than that of Maxwell Bay, and considering the wave effects, it has a significant effect on the surface flow, so it can affect the movement of particles floating on the surface layer. The lighter particles floated around the surface layer and could

travel longer, so most of them could reach the shoreline, while the denser particles sank relatively quickly and accumulated on the seabed. In addition, the wave effect increases the traveling speed of particles twice comparing to the simulation cases without the wave. It is indicated that oceanographic processes such as waves are important factors in the transport of particles that float around the surface layer in the ocean.

The present study then proposed a strategy for reducing the accumulation of particles in a specific location, which can cause more serious environmental and ecological problems. In order to reduce the concentration of microplastics in Marian Cove, it is most effective to release the wastewater before the low tide, but it was shown that the particles were accumulated near the Antarctic Specially Protected Area. Accordingly, when microplastics were released from the surface of seawater a little far from the shoreline, they were transported out to Maxwell Bay, and so no particles remain in Marian Cove or reach the Antarctic Specially Protected Area. Therefore, in determining the accumulation amount of microplastics contained in the wastewater discharged from the station, it is very critical to control the release location and release time at which the wastewater need to be released according to the tidal cycle.

Keywords: Microplastics, Waves, Tides, Antarctic Ocean, Scientific Research Station, Wastewater

***Student Number*: 2019-24281**

CONTENTS

LIST OF FIGURES

LIST OF TABLES

LIST OF ABBREVIATIONS

ACC	Antarctic Circumpolar Current
ASC	Antarctic Slope Current
CDW	Circumpolar Deep Water
LCDW	Lower Circumpolar Deep Water
MP	Microplastic
PET	Polyethylene terephthalate
PP	Polypropylene
UCDW	Upper Circumpolar Deep Water

LIST OF SYMBOLS

Latin Uppercase

C_d	Wind drag coefficient
F	Form Factor
F_ξ	Turbulent momentum flux in the ξ-direction
F_η	Turbulent momentum flux in the η-direction
$\sqrt{G_{\xi\xi}}$	Coefficient used to transform curvilinear to rectangular coordinates in the ξ-direction
$\sqrt{G_{\eta\eta}}$	Coefficient used to transform curvilinear to rectangular coordinates in the ξ-direction
H	Total water depth
M_ξ	Source or sink of the momentum in the ξ-direction
M_η	Source or sink of the momentum in the η-direction
N	Action density spectrum
P_ξ	Gradient of the hydrostatic pressure in the ξ-direction
P_η	Gradient of the hydrostatic pressure in the η-direction
R	Radius of particles
S	Source term involving energy density

U Depth-averaged velocity in the ξ-direction

U_{10} Wind velocity 10 meters above the free surface

$\mathbf{U}$ Eulerian velocity field

V Depth-averaged velocity in the η-direction

Latin Lowercase

c_x Propagation velocity in the x-direction

c_y Propagation velocity in the y-direction

c_{σ_w} Propagation velocity in the σ-direction

c_{θ_w} Propagation velocity in the θ-direction

d Depth below the reference plane

d_* Dimensionless particle diameter

$d\mathbf{X}_{adv}$ Displacement due to the advection

$d\mathbf{X}_{diff}$ Displacement due to the turbulent diffusion

$d\mathbf{X}'$ Random component

dZ_{sink} Sinking displacement due to the settling velocity

f Coriolis parameter

g Gravity acceleration

i Tidal constituent

n Total number of the tidal components

q_{in}	Local source per unit volume
q_{out}	Local sink per unit volume
t	Time
u	Fluid velocity in the ξ-direction
v	Fluid velocity in the η-direction
w	Fluid velocity in the σ-direction
w_s	Settling velocity of the particle

Greek Lowercase

ζ	Water level above the reference plane
η	Horizontal directional component in the curvilinear coordinate
θ	Angle between the wind stress direction and the η-direction
θ_w	Propagation direction
ν	Kinematic viscosity of water
ν_V	Vertical eddy viscosity
ξ	Horizontal directional component in the curvilinear coordinate
ρ_a	Density of the air
ρ_p	Density of the particle

ρ_0	Reference density of water
σ	Scaled vertical coordinate; $\sigma = \frac{(z-\zeta)}{(d+\zeta)}$
σ_w	Frequency
$\left\|\overrightarrow{\tau_s}\right\|$	Magnitude of the wind shear-stress

CHAPTER 1. INTRODUCTION

1.1 General introduction

In the year 2019, the world produced around 370 million tons of plastics (PlasticsEurope, 2020) and has wasted astronomical amounts of them. Substantial amounts of wasted plastics have been mismanaged plastics and released into the ocean. Once the plastics are introduced to the ocean, they can be broken down into small fragments with size < 5 mm called microplastics (MPs) mechanically by waves or opto-chemically by ultraviolet rays (Iwasaki et al., 2017). MPs are abundantly found in the Northern Hemisphere since they are originated mainly from the continents, but these types of plastics are also recently found in Antarctica, which was once known as the unspoiled ocean. In the past, studies on the pollution of Antarctic areas have focused on pollution by heavy metals and toxic chemicals (e.g., Chaparro et al., 2007; Curtosi et al., 2010). However, in recent years, pollution of MPs on Antarctic areas has been reported but could not change a lot from a view of marine pollution on the Antarctic Ocean. Only the degree of contamination of MPs remaining in the Antarctic Ocean is still being investigated, and the physical transport of MPs in this area is insufficiently reported.

There are two main origins of MPs in the Antarctic Ocean. One is likely outside of the Southern Ocean. Fraser et al. (2018) explained that biological materials could pass through the Antarctic Circumpolar Current from the

outside for an extended period of time. Based on this mechanism, MPs might travel across the Antarctic Circumpolar Current and penetrate into the Antarctic Shelf. Furthermore, based on the observations that the concentration of MPs contamination at high latitudes is higher than at mid-latitudes, if MPs are transported to the Antarctic Ocean, they are likely to be trapped and accumulated around Antarctica (Isobe et al., 2017). In another way, MPs can be produced in Antarctica. They can be stemmed from human activities such as the wastewater from the scientific research stations or survey vessels inside the Antarctic Ocean (Waller et al., 2017). According to Gröndahl et al. (2009), 52% of the 71 scientific research stations in Antarctica have no adequate wastewater treatment facilities. While studies on MPs originated from the outside of the Antarctic Ocean have been carried out recently including field measurements and numerical modeling, research on MPs originating from the inside of the Antarctic Ocean has not been much performed so far. Most of MPs found in the Antarctic Ocean may come from outside, but still the effects of local sources cannot be neglected.

Once MPs are released into water columns, they travel in diverse ways depending on their size, shapes, and surrounding hydrodynamic conditions such as tide, current, wave, etc. So, understanding such physical processes helps researchers to track the movement and find locations of accumulations of MPs in Antarctica. Fraser et al. (2018) took into account the Stokes drift and the eddies to simulate and track biological particles released from the outside of the Antarctic Ocean and found that such organic particulates matters can penetrate

the Antarctic Circumpolar Current and reach the interior of the Antarctic Ocean. In addition, Isobe et al. (2014) indicated that MPs could travel by utilizing the physical oceanographic processes of the ambient ocean currents even near the Antarctic areas. Even though there are not many trails that have applied Isobe et al. (2014)'s suggestions to reproduce ocean circulation, based on Fraser et al. (2018), we need to investigate the effects of the oceanographic variables such as waves and tides on the uppermost layer for more accurate tracking the transport of MPs.

In order to accurately track the travel trajectories and also find the locations for abundant accumulation of MPs, their vertical velocities must be tuned elaborately. This parameter is determined by mainly three properties of the particles: density, size, and shape. In the ocean, MPs' types, shapes, and sizes are very diverse depending on whether MPs are released directly from the source or have been degraded (Khatmullina and Isachenko, 2017). Many studies have performed experiments to define the particle's settling velocity according to the characteristics of the particle (e.g., Chubarenko et al., 2016; Khatmullina and Isachenko, 2017; Zhiyao et al., 2008). According to the previous studies, if the particles are of the same size and shape, the denser particles, the faster they sink, as we well knew. Moreover, the particles of the same density sink faster as the size increases. Thus, it is essential to consider the particles' vertical velocity for tracking MPs by numerical simulation.

Recently, research on MPs in Antarctica has been focused (Table 1.1). The wastewater from the research stations must be a very important source of MPs

even though the amount of MPs may be negligible considering the size of the Antarctic Ocean (Waller et al., 2017). However, many studies are getting more concerned about the contamination of MPs in the wastewater from the research station, based on MPs sampled around their research station (e.g., Cincinelli et al., 2017; Munari et al., 2017; Reed et al., 2018). Although they reported that how many MPs are concentrated near some stations, physical research on how they are transported is insufficient. Therefore, it is necessary first to figure out how many MPs have been accumulated near the station and then physically investigate how MPs contained in the wastewater are transported.

Accordingly, the present work also collected samples that can include MPs by conducting a field survey in Marian Cove, near the King Sejong Station, which is the Korean Antarctic research facility during January and February 2019. In addition, to find how many MPs are contained in the wastewater from the King Sejong Station, the wastewaters were also collected. Based on the sample collections, the contamination concentration of MPs in Marian Cove was found to be somewhat higher than we expected, and the wastewater contained a significant number of MPs, which is much more than the number of MPs collected from seawater.

1.2 Objectives

Previous research on MPs found near the station reported that a significant number of MPs had been found. Especially, the concentration of MPs was highest in areas potentially affected by the influence of the station (Munari et al., 2017). In fact, since MPs in Antarctica are not regularly sampled and recorded to date (Waller et al., 2017), studies on MPs pollution near the stations in each country are encouraged.

The discovery of large numbers of MPs near the scientific research stations residing in Antarctica has raised the possibility that the wastewater from the stations may be a major source of MPs contamination on a local scale. Therefore, the present work is aimed mainly to figure out the trajectories and mechanisms of the accumulation of MPs contained in the wastewater of the King Sejong Station. There are four specific goals to reach the main objective as follows:

(1) Investigating how MPs are transported according to their characteristics in Marian Cove.
(2) Understanding how the wave effect affects the trajectories of MPs in Marian Cove.
(3) Finding out whether local accumulations of MPs released from the station depend on the tidal cycle.
(4) Determining which location is optimal for reducing the MPs' accumulation in Marian Cove.

For this work, we tracked the particles by using the Lagrangian Particle Tracking method that reflects the properties of MPs. Chapter 2 describes a research background related to MPs and Antarctica, and Chapter 3 explains how this study was conducted. Chapter 4 presents the results of the four questions, and finally Chapter 5 gives a summary and conclusion.

Table 1.1. Previous and present studies on MPs

Reference	Methodology	Research area	Main purpose
Isobe et al. (2014)	Field survey & Numerical modeling for the simple case	15 stations in the western part of the Seto Island Sea, Japan	Investigating the quantity and size distribution of small plastic fragments and figuring out the selective transport of MPs
Cincinelli et al. (2017)	Field survey	Ross sea in Antarctica	Investigating the concentration of MPs
Isobe et al. (2017)	Field survey	Antarctic Ocean	Investigating the concentration of MPs
Iwasaki et al. (2017)	Field survey & Numerical modeling	Sea of Japan (East Sea)	Indicating transport of MPs considering stokes drift in the research area
Munari et al. (2017)	Field survey	Terra Nova Bay in Antarctica	Investigating the concentration of MPs in sediment near the scientific research station
Fraser et al. (2018)	Numerical modeling	Antarctic Ocean	Showing that organic matter can penetrate the ACC with eddies and stokes drift
Reed et al. (2018)	Field survey	Near Rothera research station in Antarctica	Investigating the concentration of MPs in sediment near the scientific research station
Present study (2021)	Field survey & Numerical modeling	Near the King Sejong Station in Antarctica	Investigating the concentration and trajectories of MPs contained in the wastewater discharged from the station

CHAPTER 2. RESEARCH BACKGROUNDS

2.1 Properties of microplastics

MPs found in the ocean vary widely in size, shape, and density. Generally, plastics with a size smaller than 5 mm are called microplastics (MPs). However, the minimum size of MPs is still controversial because it can be determined by the sampling method or the post-processing technique (Chubarenko et al., 2016). Moreover, if microorganisms or algae are attached to MPs in the ocean, the size of MPs can be increased.

MPs can be divided into two types: primary MPs and secondary MPs. When MPs are released directly, it is called primary MPs. And then, when the primary MPs are degraded into small fragments due to waves or ultraviolet rays, it becomes secondary MPs. In general, primary MPs have slightly regular shapes such as beads or spherules, while secondary MPs display various shapes (Khatmullina and Isachenko, 2017). Also, as the particles decompose over time, the edge of particles becomes smoother (Hidalgo-Ruz et al., 2012).

A particle in water has its intrinsic properties, resulting in a downward or upward force due to its vertical velocity. The particle's vertical velocity is one of the major factors in the movements of MPs, and it depends on the size, shape, and density. If MPs are lighter than seawater, they can have a rising velocity, and if they are denser than seawater, they can have a falling velocity. Some authors proposed the settling velocity of MPs in the water to understand the

motion of particles depending on their properties. Zhiyao et al. (2008) suggested a formula that can predict the settling velocity of sediments particles as below:

$$w_s = \frac{\nu}{2R} d_*^3 \left(38.1 + 0.93 d_*^{12/7}\right)^{-7/8} \tag{1a}$$

$$d_* = 2r \left(\frac{\left(\rho_p - \rho_w\right) g}{\rho_w \nu^2} \right)^{1/3} \tag{1b}$$

Chubarenko et al. (2016) noted that Zhiyao et al. (2008)'s formula works well for the spherical shape, but it does not fit for the fiber and flakes shapes. Khatmullina and Isachenko (2017) also suggested the settling velocity formula through laboratory experiments for the general shapes of MPs (e.g., spherical, cylindrical).

$$w_s = \frac{\pi}{2} \frac{1}{\nu} g' \frac{DL}{55.238L + 12.691} \tag{2}$$

However, these formulas have been empirically obtained by experiments, and to date, research on the settling velocity of MPs in the real ocean remains insufficient. Nevertheless, the above formulation can be applied to many studies to understand the transport of MPs in the ocean.

2.2 Microplastics remaining in the Antarctic Ocean

2.2.1 Oceanographic process in Antarctica

Antarctica is surrounded by the Antarctic Circumpolar Current (ACC), which can act as a barrier for Antarctica to be isolated. It is a deep-reaching flow from westward to the eastward of the Antarctic Ocean. Moreover, it serves to prevent warm currents from penetrating into Antarctica. The ACC estimated pathway is approximately 24,000 km, which is the longest current. Also, it is presumed to be the largest current, which can transport an average of 136.7±7.8 Sv measured across the Drake Passage (Carter et al., 2008).

The ACC is known to be unable to reach the Antarctic Shelf because it is disturbed by the clockwise-circulating subpolar gyres (e.g., Ross Gyre, Weddell Gyre) and the Antarctic Slope Current (ASC). However, there is actually the Circumpolar Deep Water (CDW) within the ACC that can be transported to the Antarctic Shelf. It is generally divided into Upper Circumpolar Deep Water (UCDW) and Lower Circumpolar Deep Water (LCDW). Both CDWs can penetrate the ACC, but UCDW is more likely to reach the Antarctic Shelf than LCDW. This is because LCDW is saltier and colder than UCDW, so it usually flows into the abyssal ocean, not flows into the Antarctic Shelf (Llanillo et al., 2019). The main currents of the Antarctic Ocean are shown in Figure 2.1.

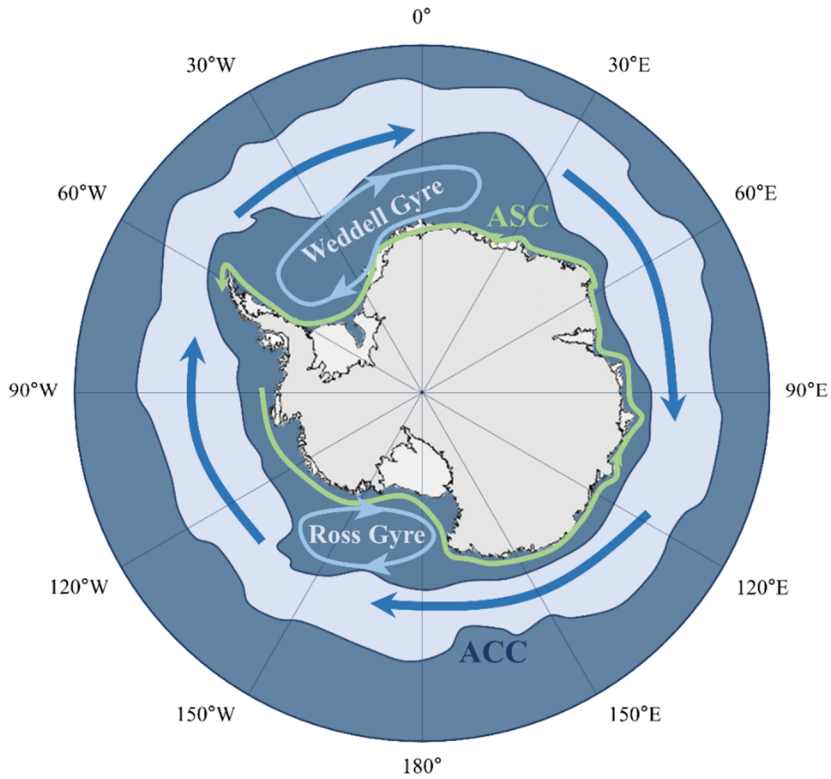

Figure 2.1 The principal oceanographic processes in Antarctica containing: the ACC, ASC, and Ross and Weddell Gyres.

2.2.2 Microplastics found in Antarctica

Previously, research on MPs was mainly focused on the heavily populated Northern Hemisphere, but recently many studies have reported the existence of numerous macroplastics and microplastics in the sparsely populated Antarctica. Based on the recent studies, the origins of MPs found in the Antarctic Ocean can be largely assumed to be twofold: outside and inside.

Antarctica is isolated from the populated areas, and it has a very small population. Fraser et al. (2018) investigated that organic particles outside Antarctica can reach Antarctica through the ACC by a transport dispersion process, which indicates that MPs can also penetrate the ACC and reach Antarctica. Furthermore, if macroplastic is transported to Antarctica, it can be degraded to microplastics owing to the oceanographic processes. Besides, Isobe et al. (2017) collected MPs around the Antarctic Ocean, and many MPs have been found there. In particular, the closer to the Antarctic Ocean, the higher the concentration of MPs, which means that if MPs are transported to the Antarctic Ocean, they could become trapped around there.

Waller et al. (2017) stated that one of the origins of MPs found in Antarctica is the wastewater of the scientific research stations residing there, and actually, many MPs were found near the stations (Figure 2.2). It is expected that the accumulation of MPs in Antarctica is due to anthropogenic impacts. Actually, more than half of the 71 scientific research stations located in Antarctica did not have adequate wastewater treatment facilities (Gröndahl et al., 2009). In addition, a few studies revealed that MPs had been found around their country's

stations in Antarctica (e.g., Cincinelli et al., 2017; Munari et al., 2017; Reed et al., 2018). Therefore, it can be considered that MPs contamination around the stations is caused by the wastewater discharged from the stations, and the wastewater can be a major source on a regional scale.

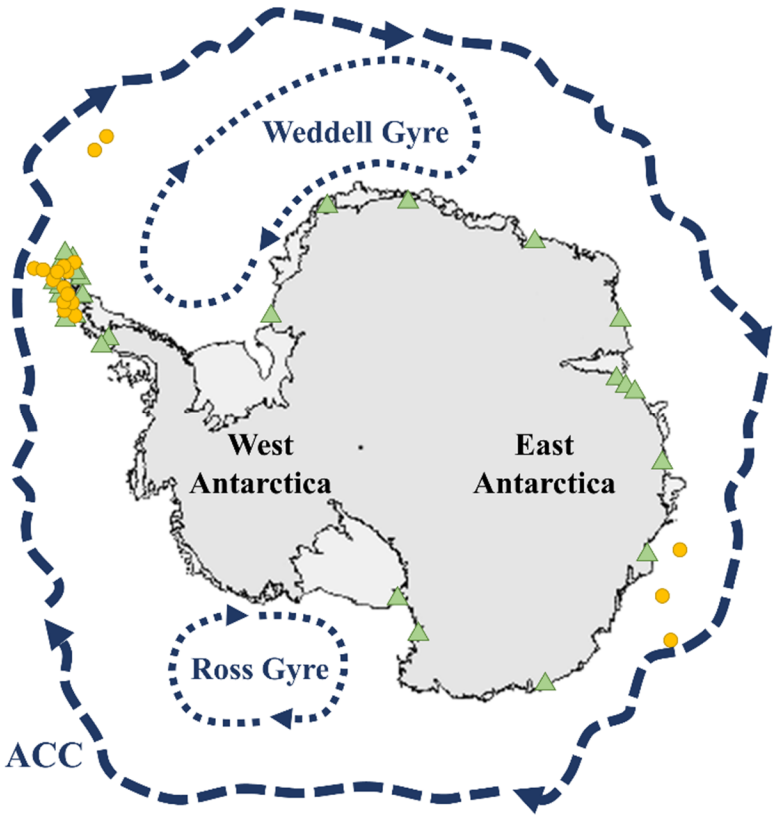

Figure 2.2 Scientific research stations (green triangles) and reported discovery of microplastics (yellow dots) (redrawing Waller et al., 2017).

2.3 Research area

At the end of the Antarctic Peninsula, Nelson Island and King George Island are separated by Maxwell Bay, which has several tributary fjords: Edgell Bay, Collins Harbour, Potter Cove, and Marian Cove (Figure 2.3(a) and (b)). The King Sejong Station is located at the mouth of Marian Cove in King George Island, which is the closest place to South America, a civilized world, and also the research stations from many other countries reside along the coastal line of Maxwell Bay. The bay is a 'U' shaped fjord, so its depth is steepening towards the center of the bay, and its longitude axis is about 14.5 km with a maximum depth of about 500 m. The main entrance toward the Bransfield Strait is located on the southeast of the bay, and there is a very shallow and narrow strait called Fildes Strait on the northwest side of the bay.

Marian Cove is one of the tributary fjords in Maxwell Bay, surrounded by the Weaver Peninsula to the north and the Barton Peninsula to the south (Figure 2.3(c)). It is about 4.4 km longitude axis, and the width of its entrance towards Maxwell Bay is about 1.5 km with a maximum depth of 130 m. According to the observation of Yoo et al. (1999), water temperature and salinity are almost uniform, and so Marian Cove is assumed to be vertically well mixed. Moreover, based on the measurement data from the Korea Polar Research Institute (KOPRI), two small sills of about 70 m depth are located at the entrance of the cove and another inside the bay, respectively (Figure 2.3(c)). The depth of the entrance sill allows the surface water of Maxwell Bay to flow freely into Marian Cove (Yoo et al., 1999), and may not significantly affect the transport of

particulate matter.

The tidal regime can be categorized with respect to a Form Factor, F, which can infer which of the diurnal and semi-diurnal tides is relatively more important. The Form Factor in the study area is about 0.7, which can be seen as semi-diurnal cycles. The Form Factor and approximately categorized tides can be expressed as follows (Pugh, 1987):

$$F = \frac{K_1 + O_1}{M_2 + S_2} \tag{3}$$

$0 < F \le 0.25$	semi-diurnal
$0.25 < F \le 1.50$	mixed, predominantly semi-diurnal
$1.50 < F \le 3.00$	mixed, predominantly diurnal
$3.00 < F$	diurnal

In this research area, a mixed semi-diurnal tide is dominant with an unusual inequality in tidal heights. The mixed semi-diurnal has a mean tidal range of 1.5 m with a maximum spring tidal range of 2.8 m (Yoo et al., 2015). This range of tidal forcing seems to be strong enough to play an important role in the exchanges of seawater between Maxwell Bay and Bransfield Strait and also between Marian Cove and Maxwell Bay (Llanillo et al., 2019). Therefore, when there is not strong wind and other forcings, the tide is regarded as the main forcing by changing the water structure in Maxwell Bay and Marian Cove.

The King Sejong Station is a research station located on the coast near the entrance of Marian Cove (62.22°S, 58.79°W in Figure 2.3(c)). About 17 researchers reside minimally in a full year in the station, and about 100 researchers stay during the austral summer. Generally, only 63 % of the stations

operated during a full year have a proper sewage treatment system (Gröndahl et al., 2009). The King Sejong Station has been equipped with a sewage treatment system to purify the domestic wastewater, which was replaced in 2008 with the old system. The newly installed purifying facility is the sewage treatment system utilizing the IC/SBR (Internal Circulation Sequence Batch Reactor) process, and this system can effectively remove pollutants such as organic matter, nitrogen, and phosphorus by alternately creating aerobic and anaerobic conditions. It was reported that the removal rate of MPs during the sewage treatment, the SBR (Sequence Batch Reactor) process treats 98% of total MPs (Lee and Kim, 2018), and so the IC/SBR may have a similar rate to the SBR. However, we are still not sure how many MPs are actually released into Marian Cove from the station. The wastewater purified through this sewage treatment system is discharged into the sea through a discharge pipe sitting in front of the research station, half-buried on the shore (Figure 2.3(d)). The discharge port is designed to release wastewater directly to the surface layer of Marian Cove and it is likely to have a direct impact on the marine environment of Marian Cove.

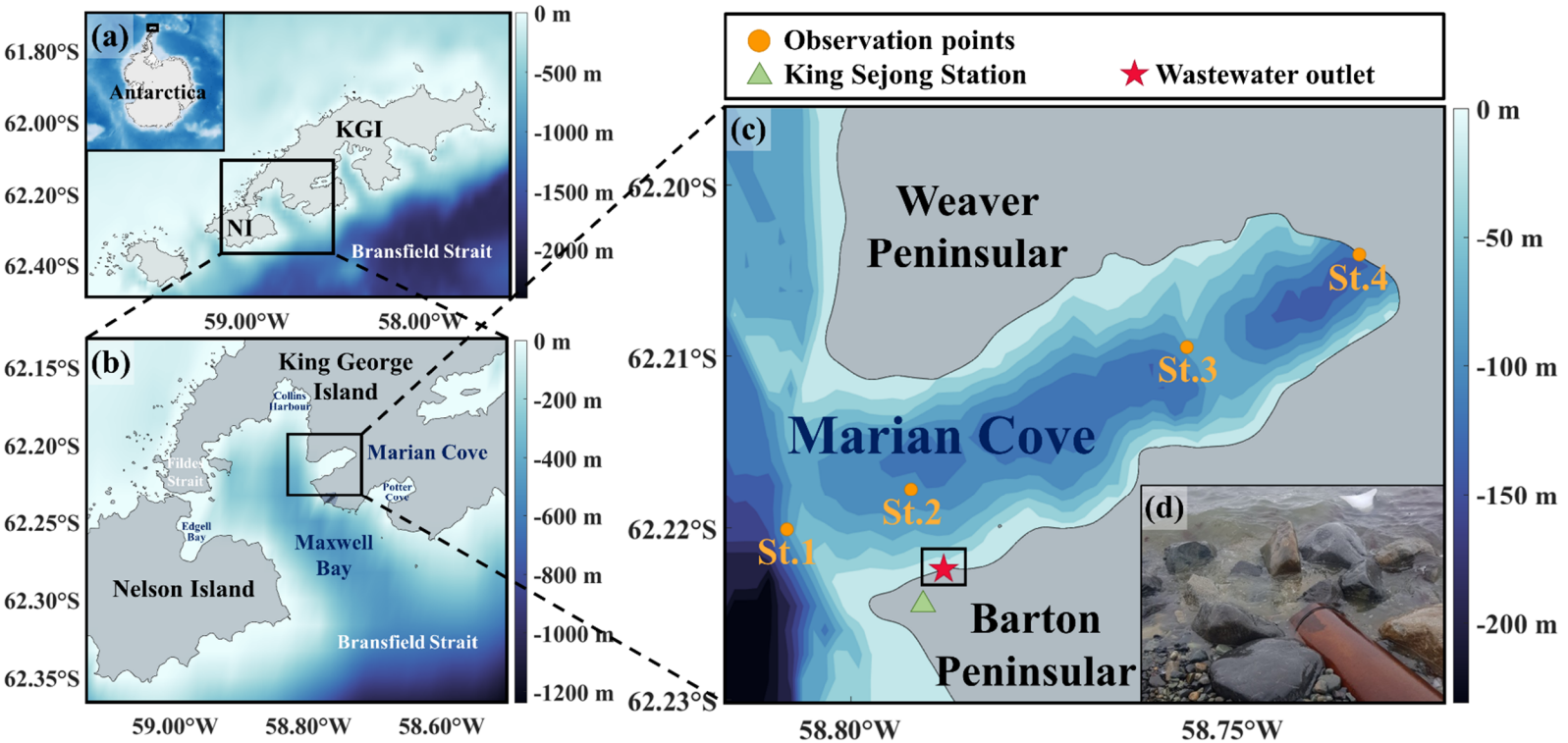

Figure 2.3 Map of (a) King George Island and Nelson Island of South Shetland Islands and (b) zoomed map of Maxwell Bay showing bathymetry by interpolating ETOPO1 data. KGI: King George Island, NI: Nelson Island. (c) Zoomed map of Marian Cove with interpolated bathymetry based on the measurement data from KOPRI and (d) the wastewater outlet of the King Sejong Station.

CHAPTER 3. METHODOLOGY

3.1 Field survey

The present work executed cooperative research with Incheon National University, and we had surveyed to sample MPs near the station during January and February 2019. The seawater was sampled in Marian Cove for two days from January 27 to January 28, 2019, and the wastewater from the King Sejong Station was collected twice on January 23 and February 4, 2019. MPs in the water column were collected in the surface, intermediate, and bottom layers of the four locations in Marian Cove, as well as the influent and effluent water from the King Sejong Station. The sampling locations are shown in Figure 2.3(c), and they are summarized in Table 3.1.

Table 3.1 Locations of the observation points and the King Sejong Station (KSS)

Observation Point	St.1	St.2	St.3	St.4	KSS
Location	62.22°S, 58.81°W	62.22°S, 58.79°W	62.21°S, 58.76°W	62.20°S, 58.73°W	62.22°S, 58.79°W

Samples were collected twice 500 L of seawater at each depth of the three layers using an underwater pump, so 24 samples were obtained for four stations. Each sample was filtered through a net having a mesh size of 20 μm to reduce the volume in the field. In addition, to avoid contamination when collecting

samples, the net was backwashed three or more times before collection to remove all substances inside the net. Samples larger than 20 μm were pre-treated, and the type, shape, and size of the particles were analyzed using a μ-FTIR microscope.

Samples of influent and effluent water from the King Sejong Station's sewage treatment plant were collected at intervals of two weeks. Since it was collected twice for each sample, eight samples were obtained with four samples of each influent and effluent water. The influent and effluent water were collected 1 L and 500 L, respectively, and the underwater pump was used to collect the effluent water. These samples were also analyzed in the same way as seawater analysis for particles larger than 20 μm.

The average concentration of MPs in Marian Cove was 120.1±101.9 particles/m^3 (Figure 3.1). The MPs concentration was highest at St.2, which is the closest to the King Sejong Station. Except for St.2, the concentration of MPs increased toward the inside of the cove. In St.2, more MPs were found toward the bottom layer, but in the rest of the stations, they were evenly distributed in the vertical direction (Figure 3.2(a)). Among them, PP dominated at all observation points, and most of them existed in the form of fragments. According to the MPs samples collected from the King Sejong Station's wastewater, the concentration of the influent was $(468\pm93)\times10^3$ particles/m^3, and that of the effluent was $(193\pm12.5) \times 10^3$ particles/m^3. The MPs concentration of the wastewater was about 1000 times higher than that of seawater, and PP and PET existing mainly in the form of fragments were

dominant. Besides, when comparing MPs found in the influent and effluent, the effluent contained MPs with 59% removed from the influent (Figure 3.2(b)).

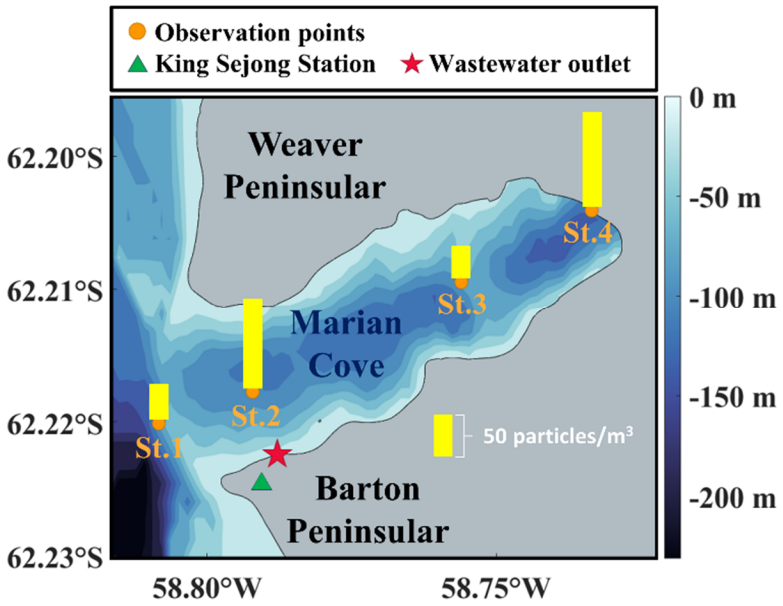

Figure 3.1 Concentration of MPs for four stations.

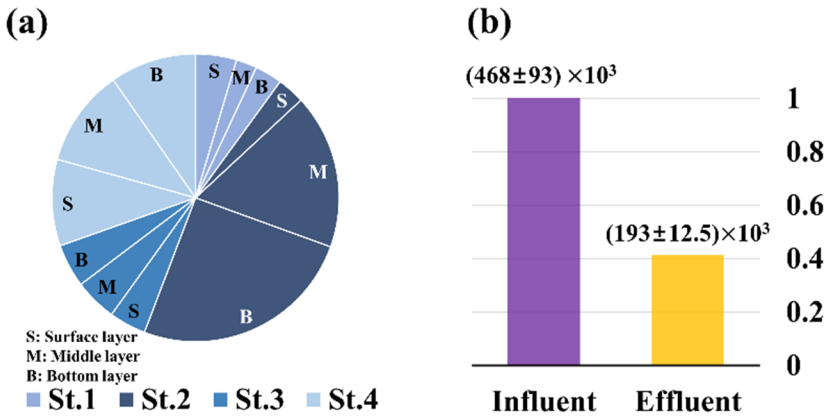

Figure 3.2 (a) The ratio of MPs collected in Marian Cove for each station and (c) for influent and effluent from the King Sejong Station.

3.2 Numerical model descriptions

3.2.1 Hydrodynamic model

Delft3D, a hydrodynamic model developed by Deltares, was used to reproduce the ocean circulation in Maxwell Bay, including Marian Cove. This numerical modeling system consists of several modules for flow, wave, sediment transport, etc., so it can simulate well, including complicated coastal lines. Each module can be carried out independently (stand-alone) or by online coupling, and this study coupled the flow and wave modules in an online way to simulate simultaneously tidal currents, waves, and other processes. The modeling system adopts the Arakawa C-grid combining orthogonal curvilinear coordinates for the horizontal grids (Deltares, 2017a), and we chose the sigma coordinates for the vertical grids. In order to close the turbulence term, this study applied the k-epsilon turbulence model to the vertical turbulent eddy viscosity and diffusivity. Unlike the standard level 2.5 turbulent closure model of Mellor and Yamada (1982), the k-epsilon model has no damping function because the effect of stratification on the mixing length is considered by the buoyancy terms of the transport equation for k and epsilon.

The flow module can predict the flow field and transport of substances. It solves the continuity equation for incompressible fluids and the Navier Stokes equations applying the shallow water and the Boussinesq assumptions. And, the vertical velocities are calculated from the continuity equation.

$$\frac{\partial \zeta}{\partial t}+\frac{1}{\sqrt{G_{\xi\xi}}\sqrt{G_{\eta\eta}}}\frac{\partial\left((d+\zeta)U\sqrt{G_{\eta\eta}}\right)}{\partial \xi}+\frac{1}{\sqrt{G_{\xi\xi}}\sqrt{G_{\eta\eta}}}\frac{\partial\left((d+\zeta)U\sqrt{G_{\xi\xi}}\right)}{\partial \eta}+\frac{\partial w}{\partial \sigma}$$
$$=(d+\zeta)(q_{in}-q_{out}) \tag{4}$$

$$\frac{\partial u}{\partial t}+\frac{u}{\sqrt{G_{\xi\xi}}}\frac{\partial u}{\partial \xi}+\frac{v}{\sqrt{G_{\eta\eta}}}\frac{\partial u}{\partial \eta}+\frac{w}{d+\zeta}\frac{\partial u}{\partial \sigma}-\frac{v^2}{\sqrt{G_{\xi\xi}}\sqrt{G_{\eta\eta}}}\frac{\partial\sqrt{G_{\eta\eta}}}{\partial \xi}$$
$$+\frac{uv}{\sqrt{G_{\xi\xi}}\sqrt{G_{\eta\eta}}}\frac{\partial\sqrt{G_{\xi\xi}}}{\partial \eta}-fv=-\frac{1}{\rho_0\sqrt{G_{\xi\xi}}}P_\xi+F_\xi+\frac{1}{(d+\zeta)^2}\frac{\partial}{\partial\sigma}\left(\nu_V\frac{\partial u}{\partial\sigma}\right)+M_\xi \tag{5a}$$

$$\frac{\partial v}{\partial t}+\frac{u}{\sqrt{G_{\xi\xi}}}\frac{\partial v}{\partial \xi}+\frac{v}{\sqrt{G_{\eta\eta}}}\frac{\partial v}{\partial \eta}+\frac{w}{d+\zeta}\frac{\partial v}{\partial \sigma}+\frac{uv}{\sqrt{G_{\xi\xi}}\sqrt{G_{\eta\eta}}}\frac{\partial\sqrt{G_{\eta\eta}}}{\partial \xi}$$
$$-\frac{u^2}{\sqrt{G_{\xi\xi}}\sqrt{G_{\eta\eta}}}\frac{\partial\sqrt{G_{\xi\xi}}}{\partial \eta}+fu=-\frac{1}{\rho_0\sqrt{G_{\eta\eta}}}P_\eta+F_\eta+\frac{1}{(d+\zeta)^2}\frac{\partial}{\partial\sigma}\left(\nu_V\frac{\partial v}{\partial\sigma}\right)+M_\eta \tag{5b}$$

Here, ξ and η are the horizontal directional component in the curvilinear coordinates, u and v are the fluid velocity in the ξ-direction and η-direction, U and V are the depth-averaged velocity in the ξ-direction and η-direction, ζ is the water level above the reference plane, d is the depth below the reference plane, and t is the time. σ is the vertical directional component, w is the vertical velocity in the σ-direction, q_{in} is the local source per unit volume, and q_{out} is the local sink per unit volume. f is the Coriolis parameter, ρ_0 is the reference density of water, P_ξ and P_η are the gradient of the hydrostatic pressure in the horizontal direction, F_ξ and F_η are the turbulent momentum flux in the horizontal direction, M_ξ and M_η are the source or sink of the momentum in the horizontal direction.

When the wind is considered, the magnitude of the wind shear stress is defined by following quadratic formulation as:

$$\left|\overrightarrow{\tau_s}\right| = \rho_a C_d U_{10}^2 \tag{6}$$

where ρ_a is the density of the air, C_d is the wind drag coefficient, and U_{10} is the wind velocity 10 meters above the free surface. Thus, the free surface boundary conditions are:

$$\left.\frac{\nu_V}{H}\frac{\partial u}{\partial \sigma}\right|_{\sigma=0} = \frac{1}{\rho_0}\left|\overrightarrow{\tau_s}\right|\cos(\theta) \tag{7a}$$

$$\left.\frac{\nu_V}{H}\frac{\partial v}{\partial \sigma}\right|_{\sigma=0} = \frac{1}{\rho_0}\left|\overrightarrow{\tau_s}\right|\sin(\theta) \tag{7b}$$

where ν_V is the vertical eddy viscosity, H is the total water depth, and θ is the angle between the wind stress direction and the η-direction grid line. More detailed information about Delft3D-FLOW is described in Deltares (2017a).

Delft3D-WAVE is the short-wave model based on a third-generation Simulating WAves Nearshore (SWAN) model to simulate the evolution of the wind-generated waves. It solves the wave action balance equation (Eq. (3)) in a two-dimensional horizontal direction. The evolution of the wave spectrum for Cartesian coordinates is expressed as follows:

$$\frac{\partial}{\partial t}N + \frac{\partial}{\partial x}c_x N + \frac{\partial}{\partial y}c_y N + \frac{\partial}{\partial \sigma_w}c_{\sigma_w} N + \frac{\partial}{\partial \theta_w}c_{\theta_w} N = \frac{S}{\sigma_w} \tag{8}$$

Here, $N(\sigma,\theta)$ is the action density spectrum, c_x, c_y, c_{σ_w}, and c_{θ_w} are the propagation velocity in the x-, y-, σ_w-, and θ_w-space, respectively.

σ_w is the frequency observed in a frame of reference moving with current velocity and θ_w is the propagation direction that is normal to the wave crest of each spectral component. S represents the source term involving energy density. The locations of the grids are defined with respect to the curvilinear coordinates in Figure 3.3. More details are given in Delft3D-WAVE manual (Deltares, 2017b).

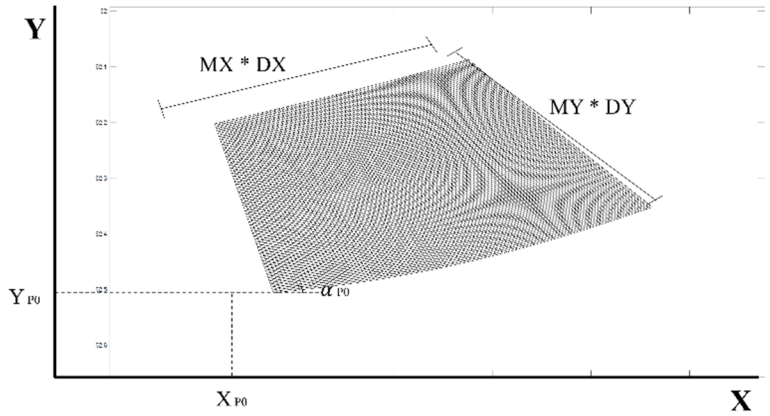

Figure 3.3 Definition of the grid in Delft3D-WAVE.

3.2.2 Microplastic tracking model

For tracing the trajectories of MPs, the present work used the Track Marine Plastic Debris (TrackMPD), which is a 3D numerical transport model developed by Jalón-Rojas et al. (2019). This tool adopts the Lagrangian Particle Tracking method that simulates the locations and speeds of MPs in consideration of their properties (density, size, and shape) by using the stored velocity field from the various ocean circulation considering the physical

processes such as advection, diffusion, sinking, etc. Based on the velocity field of the hydrodynamic model, the locations of particles are determined by taking into account the advection, diffusion, and sinking. The general equations of the particle's location are as follows:

$$\begin{aligned} X(t+\Delta t) &= X(t) + dX_{adv}(t) + dX_{diff}(t) \\ &= X(t) + U(x,y,z,t)\Delta t + R\sqrt{2K_h \Delta t} \end{aligned} \tag{9a}$$

$$\begin{aligned} Y(t+\Delta t) &= Y(t) + dY_{adv}(t) + dY_{diff}(t) \\ &= Y(t) + V(x,y,z,t)\Delta t + R\sqrt{2K_h \Delta t} \end{aligned} \tag{9b}$$

$$\begin{aligned} Z(t+\Delta t) &= Z(t) + dZ_{adv}(t) + dZ_{diff}(t) + dZ_{sink}(t) \\ &= Z(t) + W(x,y,z,t)\Delta t + R\sqrt{2K_v \Delta t} + w_s(t)\Delta t \end{aligned} \tag{9c}$$

where $d\mathbf{X}_{adv} = (dX_{adv}, dY_{adv}, dZ_{adv})$ and $d\mathbf{X}_{diff} = (dX_{diff}, dY_{diff}, dZ_{diff})$ are the displacement owing to the advection and turbulence diffusion, respectively. dZ_{sink} is the sinking displacement caused by the particles' vertical velocity w_s. $\mathbf{K} = (K_h, K_h, K_v)$ is the diffusion coefficient, where K_h is the horizontal diffusion coefficient and K_v is the vertical one. Herein, the diffusion coefficient is specified as a constant with the same order as calculated by the turbulence closure model of the hydrodynamic model.

In the process of calculating the advection, an explicit Runge-Kutta scheme of order 4/5 in space and time is used. It solves the Eulerian velocity field $\mathbf{U} = (U,V,W)$ saved from the hydrodynamic model using iterations. A random-walk model is applied to reproduce the turbulent particle motion,

where R is a random number with a mean of zero and a standard deviation of one for each time step. Herein, the diffusivity is considered in both horizontal and vertical directions.

The settling velocity that affects the vertical displacement is determined by user-defined values or computed according to the falling properties of MPs in the TrackMPD. For the spherical MPs, the settling velocity is calculated by Zhiyao et al. (2008)'s formula.

$$w_s = \frac{\nu}{2R} d_*^3 \left(38.1 + 0.93 d_*^{12/7}\right)^{-7/8} \tag{10}$$

where $d_* = 2r\left(\frac{\left(\rho_p - \rho_w\right)g}{\rho_w \nu^2}\right)^{1/3}$ is the dimensionless particle diameter, r is the radius of particles, ρ_p is the particle density, ρ_w is the density of water, ν is the water kinematic viscosity, and g is the gravity acceleration.

3.3 Numerical experiment setup

3.3.1 Computer performance

The cluster server called ARA00 in the Flow Physics and Informatics Laboratory at the Seoul National University was used for the numerical experiments. Its operating system is CentOS Linux version 6.8. And the gcc version 4.9.4 was used for compiling, and MPICH version 3.1.4 was used for parallel computing. The specification of the cluster server is summarized in Table 3.2.

Table 3.2 Cluster server specification

OS	CentOS Linux version 6.8
Compiler	gcc version 4.9.4
Parallel Computing	MPICH version 3.1.4
DELL PowerEdge R730 (ARA00)	Intel E5 2680 v4 14 Core 2.4 GHz 35MB Cache × 2 P
	128 GB DDR4 2400 (16 EA × 8 GB)
	300 GB SAS 15 K Disk × 2 EA (Mirror)
	8 TB SAS 7.2 K Disk × 4 EA (Data)

The hydrodynamic model, which is Delft3D version 4.03.01, was used for the numerical hydrodynamic experiments. The RGFGRID module embedded in Delft3D was used to generate the grid. For optimization, we conducted the parallel testing for one day. As a result, 12 cores were used using mpi (Figure

3.4). For reproducing a month, the total CPU time is about three days (250673 sec). Also, the time step is 3 seconds (0.05 min), and the saving interval is 30 minutes.

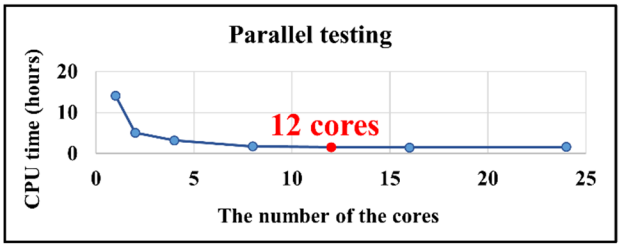

Figure 3.4 Parallel testing.

3.3.2 Hydrodynamic model setup

The flow and the wave model were coupled to figure out how MPs are migrated in consideration of the wave effects. In the hydrodynamic model, various oceanographic variables were set at the boundary as input data. All input data sources for the model experiments are summarized in Table 3.3. As already discussed in the previous section, the flow and wave models are coupled in an online way to see an interaction between current and wave in this study. Once the wave-current model produces hydrodynamic fields, the results are used to trace the locations of MPs by the Lagrangian Particle Tracking method. The shape, size, and density of particles and the initial locations are set for the input conditions. The numerical experiment follows a schematic diagram in Figure 3.5.

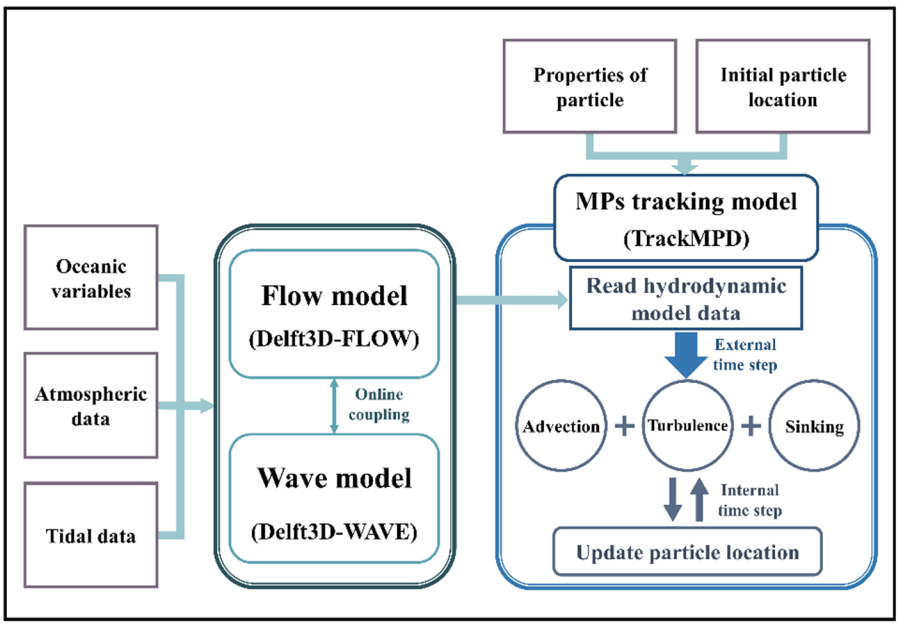

Figure 3.5 Schematic diagram for numerical experiment.

Table 3.3 Input data sources

Variable	Global model	Source	Inform.
Bathymetry	ETOPO1: Global 1 Arc-Minute Elevation	https://www.ngdc.noaa.gov/mgg/global/	- Resolution: 1 arc-minute
	KOPRI (Korea Polar Research Institute)	KOPRI	- Echosounder observation data in Marian Cove
Temperature Salinity	HYCOM (Hybrid Coordinate Ocean Model)	https://www.hycom.org/data/glba0pt08/expt-91pt2	- Vertical layer: 33 - Resolution: 1/12 degree - Updating time: 12 hours
Tide	NAO 99.b tidal prediction system	https://www.miz.nao.ac.jp/staffs/nao99/index_En.html	- Vertical layer: 33 - Resolution: 0.5 degree
Wind	CFSv2 (Climate Forecast System version 2)	https://rda.ucar.edu/datasets/ds094.0/	- Vertical layer: 33 - Resolution: 0.2 degree - Updating time: 6 hours
Wave	NWW3 (Noaa Wave Watch 3)	https://polar.ncep.noaa.gov/waves/	- Resolution: 30 arc-minute - Updating time: 3 hours

In order to construct the initial and boundary conditions of a small area near Marian Cove, the present work performed two times of nesting to increase the resolutions. The first nesting was conducted to construct the boundary condition of the interim modeling for a regional domain by interpolating data from the global scale (Figure 3.6(a) and (b)). The second nesting was performed to construct the boundary condition of the highly resolved coastal model with the data obtained from the results of the interim model (Figure 3.6(c) and (d)). The interim regional model domain ranged from 58.50°W to 59.10°W longitude and from 62.15°S to 62.50°S latitude (Figure 3.6(a)). Its longitude axis is about 31.8 km, and the latitude axis is about 38 km. It consists of a grid ranging from 250 m to 380 m in the horizontal and 10 sigma layers in the vertical directions. The detailed model domain ranged from 58.63°W to 59.00°W longitude and from 62.15°S to 62.30°S latitude, covering Maxwell Bay (Figure 3.6(c)). The horizontal grid size ranged from 120 m to 160 m. The boundary conditions were interpolated through nesting from the interim model.

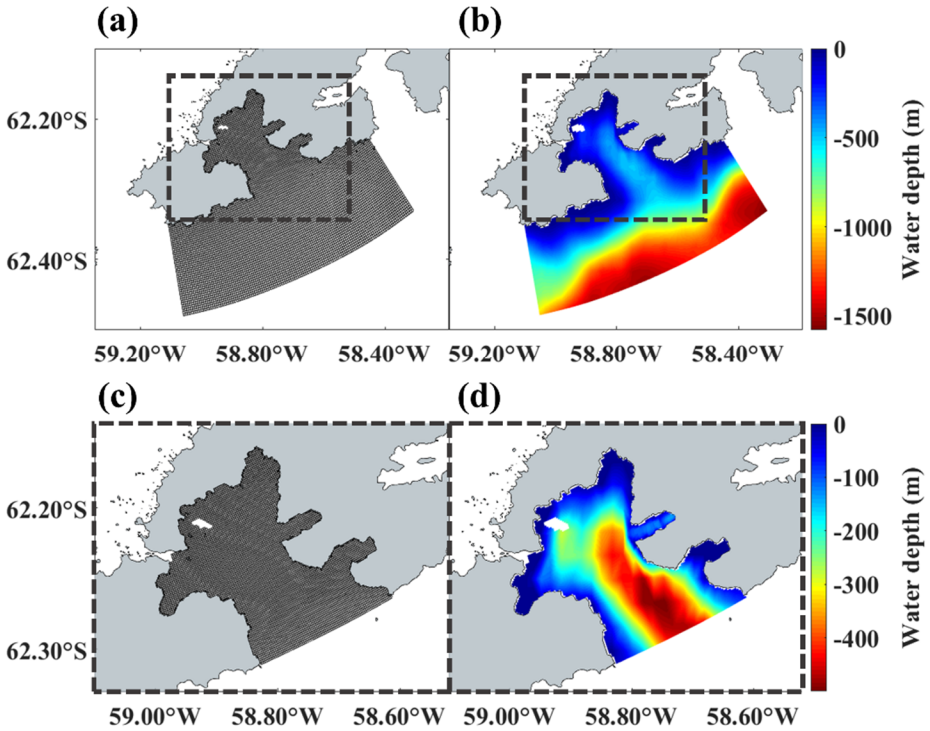

Figure 3.6 The grid [(a), (c)] and bathymetry [(b), (d)] of the first nested [(a), (b)] and the second nested [(c), (d)] flow model domains.

The bathymetry of the area was interpolated from ETOPO1, which is a global relief model that integrates land topography and ocean bathymetry with a 1 arc-minute size, and Marian Cove's bathymetry was detailed interpolated from the observation data measured by KOPRI (Figure 3.6(b) and (d)). The HYbrid Coordinate Ocean Model (HYCOM) with a resolution of 1/12° was used to construct the open boundary conditions for currents, water temperature, and salinity. Seven tidal constituents (M2, S2, K1, O1, Q1, P1, and N2) from the global ocean tide model, NAO.99b, were assigned to the open boundary. Two semi-diurnals of M2 and S2 have amplitudes of each 43.5 cm and 24.5 cm with the phases of 282° and 334°, respectively. Diurnals of K1 and O1 have amplitudes of each 23.7 cm and 25 cm with the phases of 68° and 53°, respectively, and those large scale information is also used to validate the final model results after two times nesting (Figure 4.1). In addition, the Climate Forecast System version 2 (CFSv2) was used for wind forcing. The mean wind speed and direction were 6.96 m/s and 174.5°, respectively (Figure 3.7(a)).

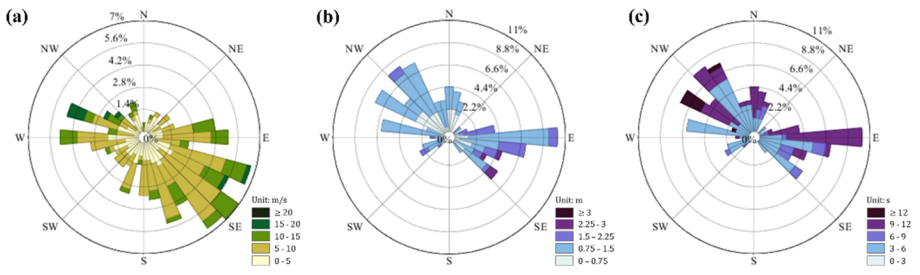

Figure 3.7 (a) The wind rose, (b) wave roses of significant wave height, and (c) mean period time for input data during the simulation period.

The wave model domain was set much larger than the flow domain to prevent the wave reflection from hindering the flow at the boundary (Figure 3.8). The grid for the wave model ranged from 280 m to 400 m. At the open boundary, a significant wave height, a primary wave mean period, and a wave direction were assigned, which were obtained from the Wave Watch III of the National Oceanic and Atmospheric Administration (NOAA) and National Centers for Environmental Prediction (NCEP). The mean significant height is 1.04 m, and the mean of the mean period time is 6.7 seconds, as shown in Figure 3.7(b) and (c).

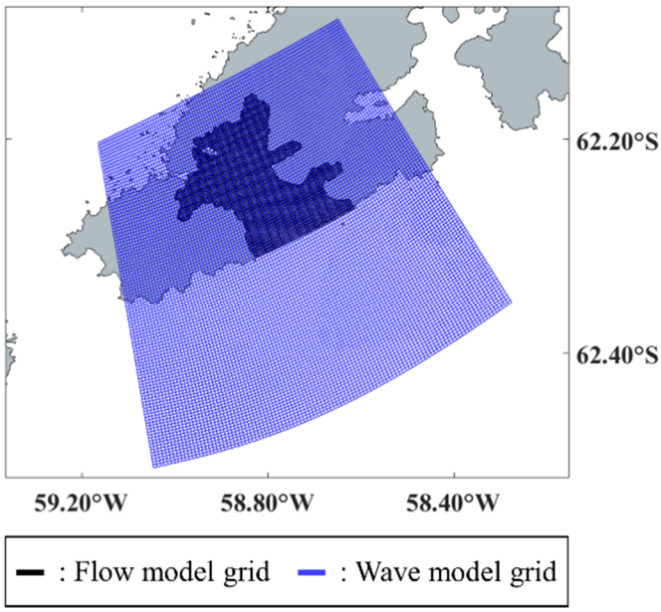

Figure 3.8 The wave model grid used when coupling with the flow model.

3.3.3 Microplastic tracking model setup

Based on the observation data of the present work, two types of MPs were found dominantly in Marian Cove and so chosen for simulation: PP and PET. And since most of MPs have a form of fragments, they were considered as spherical. While PP (0.92 g/cm^3) has a lower density than seawater, PET (1.38 g/cm^3) has a higher density, and so PP and PET move differently in the same seawater due to the difference in the particle's vertical velocity. In the TrackMPD, the settling velocity of spherical particles can be calculated according to the density and size of the particle by the equation presented by Zhiyao et al. (2008). But, if the particle's density is smaller than 1 g/cm^3, the particle is considered to move almost similar to the surface water particles. Table 3.4 shows the vertical velocities of each MP used in this experiment.

MPs tracking experiments were purposed to investigate which factor determines the accumulation of MPs in Marian Cove dominantly. Therefore, the particles were released from King Sejong Station to reproduce the behavior of MPs contained in the wastewater, and we tried to find out how waves affect the MPs' trajectory. And then, an experiment was set up to see the effect of the tidal cycle when wastewater is released on MPs' accumulation in Marian Cove. Particles were released every hour for a total of 9 hours to include the flood and ebb. Finally, the trajectories of particles depending on the releasing locations were investigated in the simulation.

Table 3.4 MPs' properties and particle's vertical velocity

Plastic class	Density (g/cm^3)	Size (μm)	Shape	Particle's vertical velocity (m/s)
Polypropylene (PP)	0.92	100	spherical	2.4×10^{-4}
Polyethylene terephthalate (PET)	1.38	100	spherical	-8.23×10^{-4}

In order to determine whether the particle's vertical velocity is small enough to be neglected compared to the vertical velocity of the flow, a dimensionless parameter named HK angle is proposed by this work. The magnitudes of vertical flow velocity are spatially very various, so this angle helps us to see the relative buoyant force, which means that the particle is falling, rising, or neutral. This dimensionless parameter is expressed as

$$\theta_{HK} \equiv \tan^{-1}\left(\frac{w_s}{W}\right) \tag{11}$$

$0 < \theta_{HK} \le \frac{\pi}{4}$ rising or falling due to W

$\frac{\pi}{4} < \theta_{HK} \le \frac{3\pi}{4}$ rising or falling due to w_s

$\frac{3\pi}{4} < \theta_{HK} \le \pi$ falling or rising due to W

where W is the Eulerian vertical velocity of the flow and w_s is the vertical velocity of the particle. The HK angle is determined by the particle's vertical velocity vector to the vertical velocity of the flow. The HK diagram is schematized in Figure 3.9. This diagram shows the dominant force contributing

to particle migration according to the HK angle.

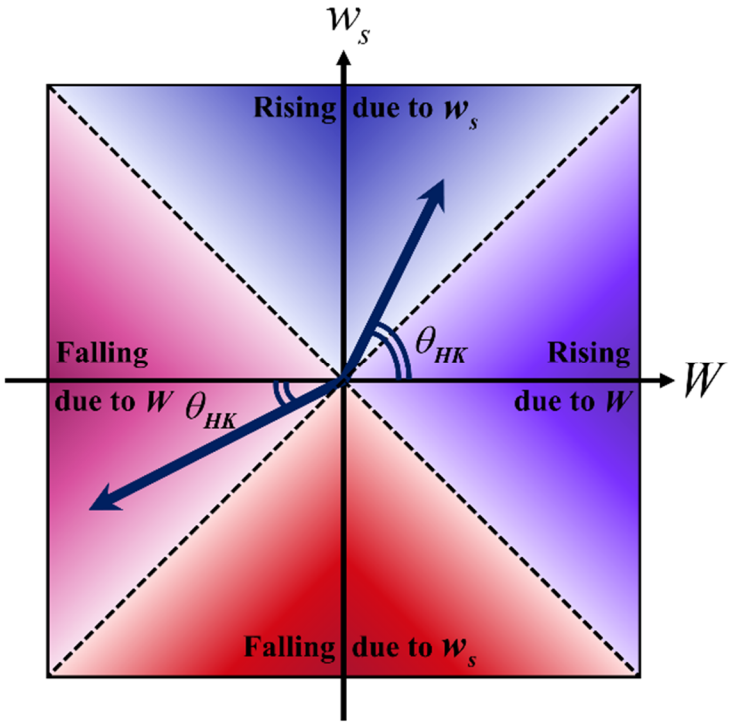

Figure 3.9 Classification of dominant force on particles according to HK number

CHAPTER 4. RESULTS AND DISCUSSION

4.1 Hydrodynamic characteristic

4.1.1 Water circulation in Marian Cove

We performed experiments to explain a mechanism for transport and accumulation of MPs, so we have not sought to verify the realism of the model in detail like in operational forecasting. Also, due to the specificity of the study area, observational data are very scarcely publicized, and the field survey conducted by the present work also was done in a very short period. We nevertheless thought it prudent to check that our results were in line with given observations and available public data.

The tidal amplitude and phase from the model results were compared to the global ocean tide model, NAO 99.b. With T_TIDE by Pawlowicz et al. (2002), the amplitude and phase were analyzed, and the results of the hydrodynamic model are compared in Figure 4.1(a) and (b). The root mean square deviations (RMSD) of the amplitude and phase were 1.29 cm and 4.61°, respectively. The RMSD was determined as follows:

$$RMSD = \sqrt{\frac{1}{n}\sum_{i=1}^{n}\left(Global\ Ocean\ Tidal\ Model_i - Model_i\right)^2} \quad (12)$$

where n is the total number of the tidal components and i is each tidal constituent.

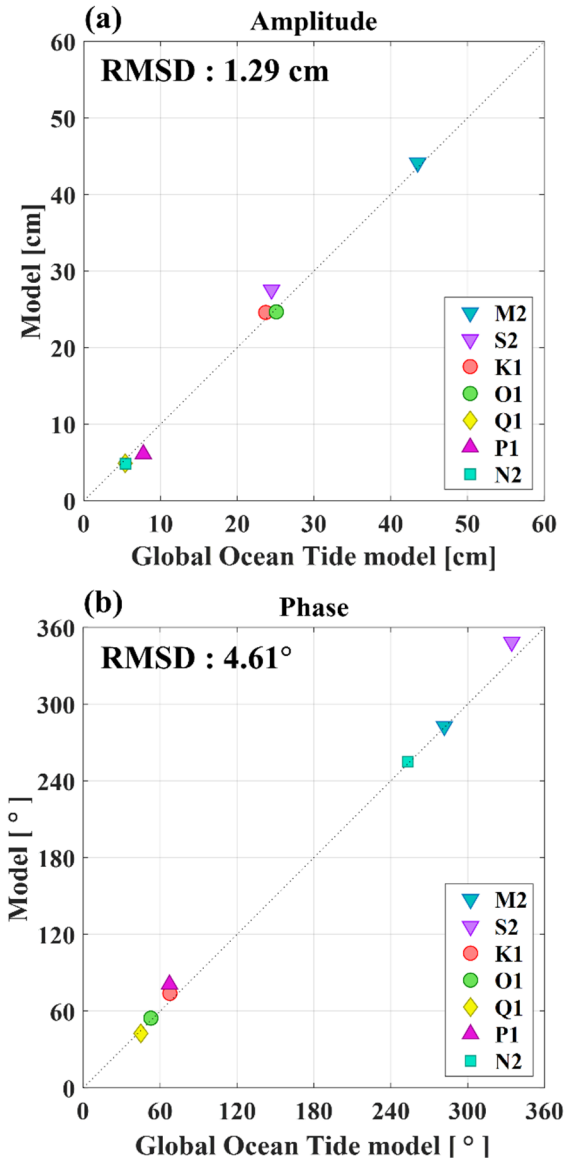

Figure 4.1 Comparison of (a) tidal amplitude and (b) phase between the model and the global ocean tide model.

The hydrodynamic experiment results are shown in Figure 4.2. The significant wave height and mean period time are 0.3 m and 1.6 seconds, respectively (Figure 4.2(b) and (c)). Since Marian Cove is a tributary of Maxwell Bay, when the wave coming from the open boundary located on the Bransfield Strait reaches Marian Cove, it has smaller values than the input data. In the case of waves, since there is no observation data to be compared and the resolution of the global wave model is too low to correspond to the research area, it is uncertain whether the results are close to the real ones. Therefore, this study only explains how the transport of MPs changes due to the influence of the wave rather than forecast the exact wave weather.

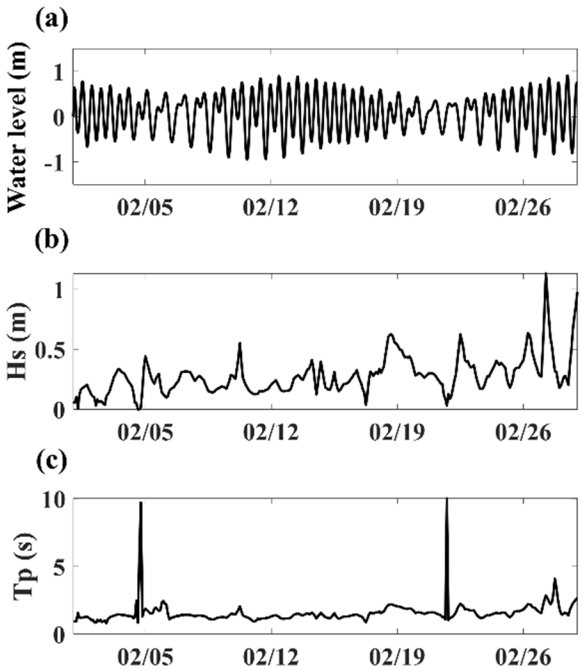

Figure 4.2 Hydrodynamic experiments results: (a) water level, (b) significant wave height, and (c) mean time period at Marian Cove.

As shown in Figure 4.3, the currents in Marian Cove are relatively slower than in Maxwell Bay. When the wave is not considered in low tide, the surface current of Marian cove circulates counterclockwise near the entrance sill due to the strong flow in Maxwell Bay, which is not observed in the case with the wave. The surface flow velocities in Marian Cove are 0.017 m/s without waves and increase to 0.023 m/s with waves toward Maxwell Bay. In the high tide, the surface current generally flows toward the northeast in Marian Cove (Figure 4.3(b)). The surface flow velocities in Marian Cove are 0.04 m/s without waves and 0.09 m/s with waves. The bottom currents are relatively slower than the surface currents with about 0.014 m/s, regardless of waves (Figure 4.3(c)). It indicates that the wave affects surface flow significantly during whole tidal periods, and so it could result in the movement of floating particles. The changes due to the waves are described in detail by the trajectories of MPs in the following section.

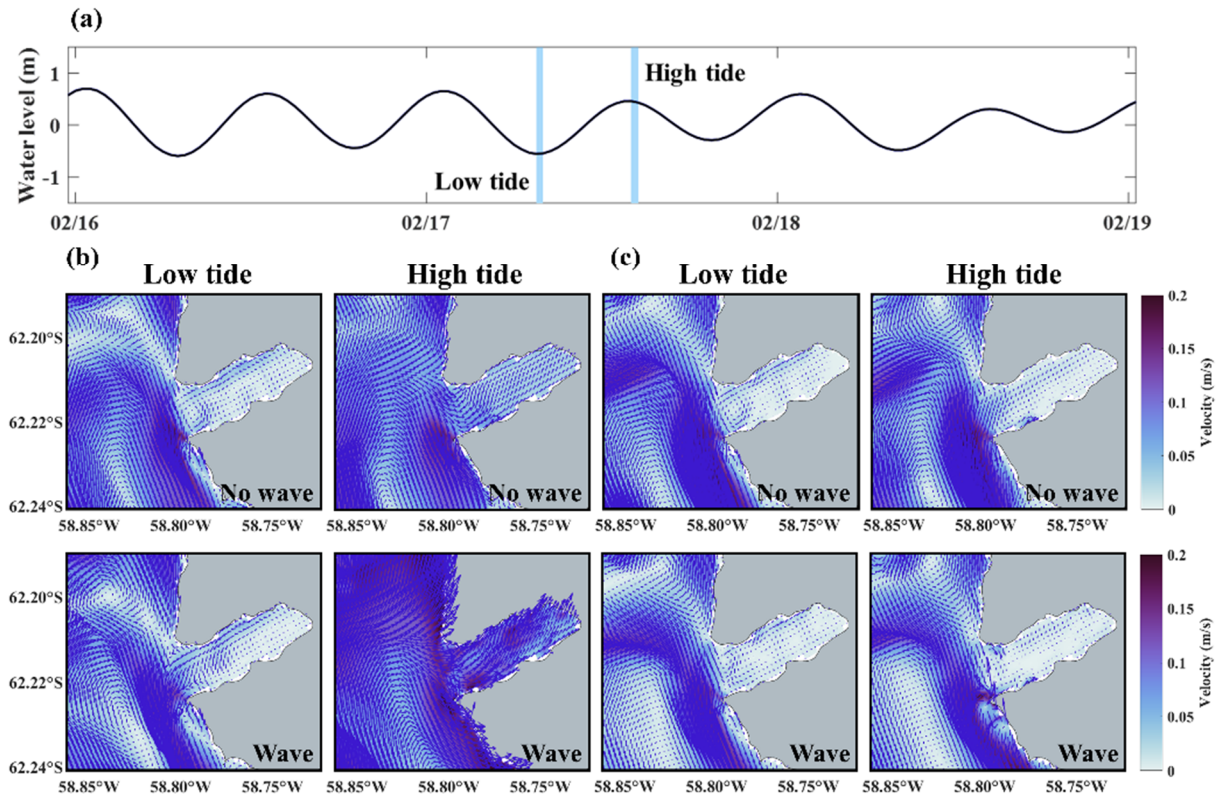

Figure 4.3 (b) Surface layer current and (c) bottom layer current around Marian Cove according to waves at the low tide and the high tide shown in (a) the water level.

4.1.2 HK angles for MPs

The HK angles for each MPs are calculated in order to figure out by what force the particles are transported in Marian Cove. It is obtained for the surface, intermediate, and bottom layer using the averaged vertical flow velocity over a day. In general, the vertical velocity in Marian Cove is not as fast as the order of 10^{-5}.

The HK angle for PP shows that the particles tend to mainly rise after they were released from the surface water, and so they can be transported along the surface layer (Figure 4.4(a)). However, one thing to note is that some points where the falling force is comparatively dominant in the surface layer, PPs can sink due to the downwelling vertical velocity of seawater. So, if they reach the innermost part (around 62.2°S, 58.75°W) or the entrance of the cove (around 62.22°S, 58.8°W), they can sink fast along with the high downward flow. Even in the intermediate layer, the buoyancy of PP is usually dominant, but the falling force in the north and the innermost part of the cove can cause the particles to sink. If the particles settle into the bottom layer, it is difficult for them to resuspend due to the relatively strong downward flow.

On the other hand, the HK angle for PET indicates that when the particles were released from the surface water in Marian Cove, they can sink due to their falling velocity (Figure 4.4(b)). In the intermediate layer, the particles can still sink due to their falling velocity, and the downward vertical velocity of seawater is strong at some points of Marian Cove. However, if the particles move to Maxwell Bay, the upward vertical velocity of seawater is strong, and so they

can rise. When particles reach the bottom layer, except in a few points, most of them cannot rise due to their falling velocity and downwelling flow, except at some locations around the coast.

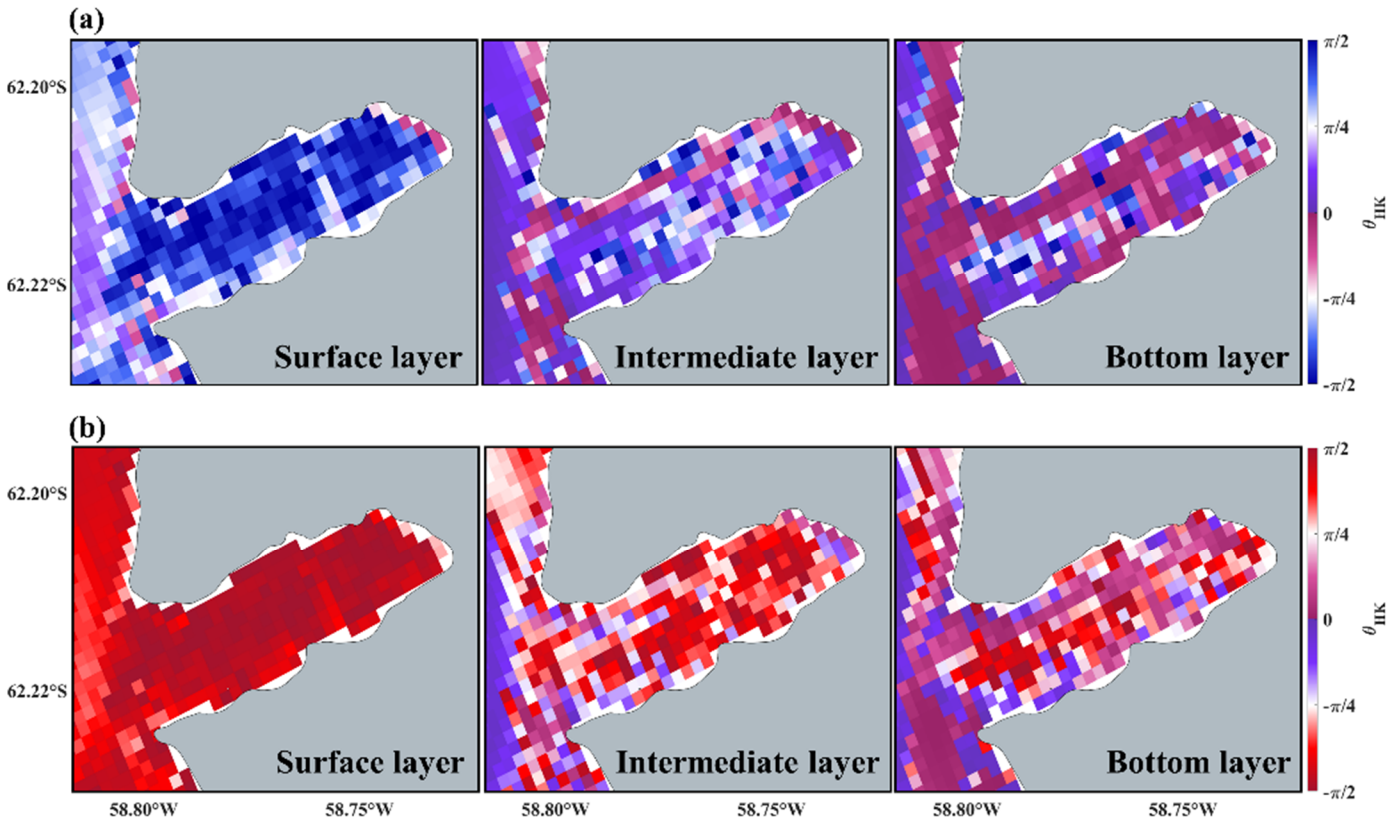

Figure 4.4 HK angle for (a) PP and (b) PET with respect to the surface, intermediate, and bottom layer surrounding Marian Cove.

4.2 Impact of waves on the trajectory of MPs

To investigate the effects of waves on the transport of MPs contained in the wastewater discharged into the surface water, 20 of each polymer were released from the location of the wastewater outlet of King Sejong Station. Comparing the migration trajectories of PP and PET each other, PPs are lighter and so transported further inside Marian Cove than the denser particles, PETs (Figure 4.5(a) and (c)). With the HK angle for PP, most of them tend to float around the surface layer due to buoyancy and reach the shoreline within a day. In the case with the wave, some PPs reach in front of the glacier coast at Marian Cove, and they sink rapidly due to the high downward flow (Figure 4.5(b)).

On the contrary, PETs have the HK angle implying the particle's falling velocity is dominant in the surface layer of Marian Cove, and so they sink into the intermediate layer just after releasing particles and tend to travel along with its flow to Maxwell Bay (Figure 4.5(c)). When considering waves, the trajectories of MPs in the lower layer are changed, and particles tend to be not transported out to Maxwell Bay but stay inside Marian Cove (Figure 4.5(d)). It means that waves made the water body in the lower layer circulate in a clockwise direction near the entrance of Marian Cove, and thus particles tend to stay inside Marian Cove.

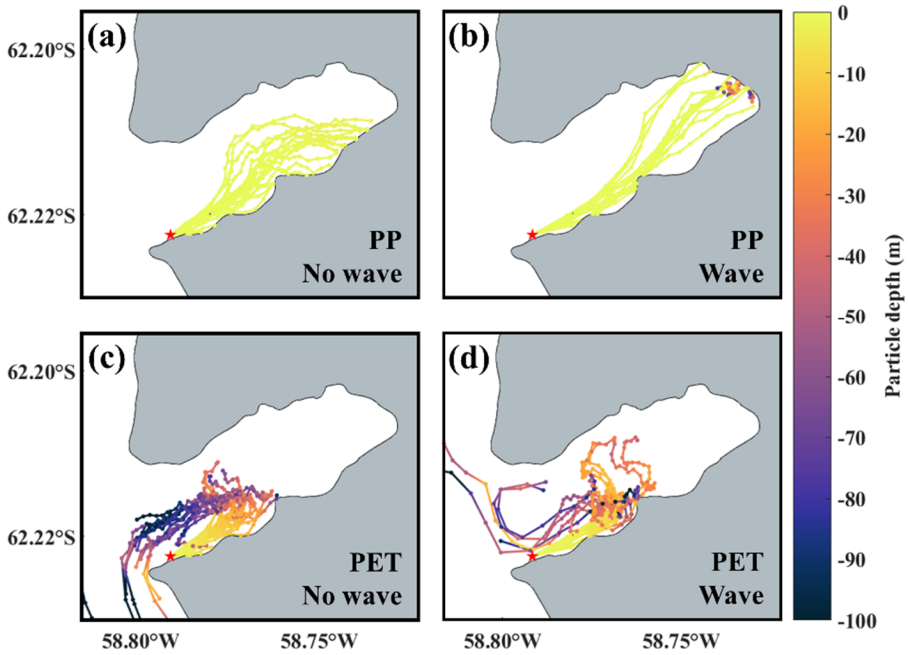

Figure 4.5 Comparison of horizontal Lagrangian Particle Tracking between PP [(a), (b)] and PET [(c), (d)] released from the wastewater of the King Sejong Station: No wave [(a), (c)] and with wave [(b), (d)].

The travel distance and time of each MP are compared according to the wave existence (Table 4.1). Just after particles were released near the shoreline, some particles land on the shoreline very shortly. Thus, the average travel distance was calculated only for particles that did not land within 6 hours, and the average travel time was also computed for particles that traveled 1 km. Waves made PP and PET travel by about 830 m and 460 m further, respectively. And the travel speed of both types of MPs is almost twice the case without waves (Table 4.1). Comparing the number of MPs remained in Marian Cove, all PPs remained in the cove, regardless of the effect of the waves. On the other hand, when the wave effect is not considered, 30% of the particles were transferred out to Maxwell Bay, while when the wave effect is considered, 10% of the particles were transported to Maxwell Bay out (Figure 4.6). It is indicated that the wave forces the particles to travel to inside Marian Cove. As a result, waves must significantly affect the travels of particles in the extended regional level and local Marian Cove scale by changing the direction of the flow. Therefore, it is an essential factor to consider in order to track the trajectories of MPs.

Table 4.1 The average of the travel distance and the average of the travel time

	PP without wave	PP with wave	PET without wave	PET with wave
The number of particles used in the calculation	18	12	18	15
Travel distance for 6 hours	1100.1 m	1929.2 m	1022.4 m	1485.7 m
Travel time for 1 km	5 hours	2.8 hours	5.4 hours	2.9 hours

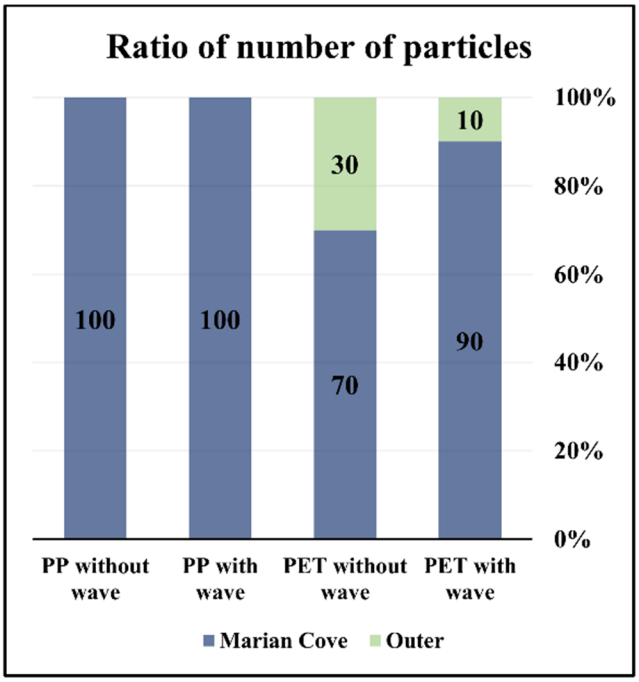

Figure 4.6 Ratio of the number of remaining particles.

4.3 MPs' trajectories depending on releasing time

In Maxwell Bay and its tributary fjords, tides play a major role in the circulation of the water body. Also, tides contribute significantly to the transport water mass between Maxwell Bay and Marian Cove (Llanillo et al., 2019). Therefore, the transport of particles must be affected by tides, and their behavior strongly depends on the releasing time in the tidal period. Thus, the transport characteristics of each MP were investigated by releasing 100 particles according to the different tidal times. Particles were released with intervals of one hour including flood and ebb times, and the times to release particles are shown in Figure 4.7.

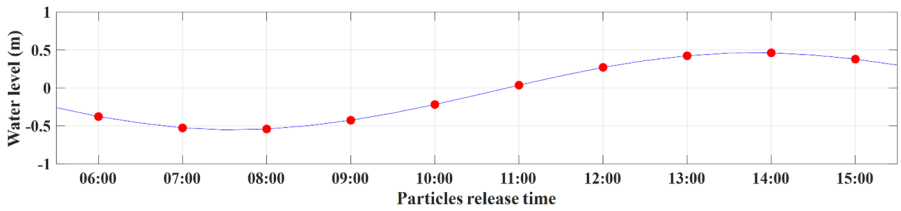

Figure 4.7 Particles releasing time expressed in the water level location.

Most of PPs tend to easily flow into the interior of Marian Cove along the surface currents, except at 06:00, the ebb time (Figure 4.8). When the particles reach near the glacier, they quickly sink toward the bottom layers due to the downwelling current. And then, they tend to circulate clockwise in the intermediate layer of Marian Cove. Most of the particles were deposited or landed within Marian Cove, but a few particles escaped from Marian Cove and

traveled out to Maxwell Bay.

All PETs also moved out to Maxwell Bay like PP during the ebb time, 06:00 (Figure 4.9). However, during the flood time, the speed of PET entering the interior of Marian Cove was much smaller than PP since PET has a faster falling velocity. Thus, PETs move to the intermediate layer quickly just after they were released and so were transported mainly by the current in that layer. When both polymers float around the intermediate layer circulating clockwise near the entrance of the cove, there is a slight chance of transporting into Maxwell Bay. When particles were released at 8:00, which is the low tide, the velocity near the releasing point slowed down to about 0.01 m/s, so the particles tended to stay near the releasing point (Figure 4.9).

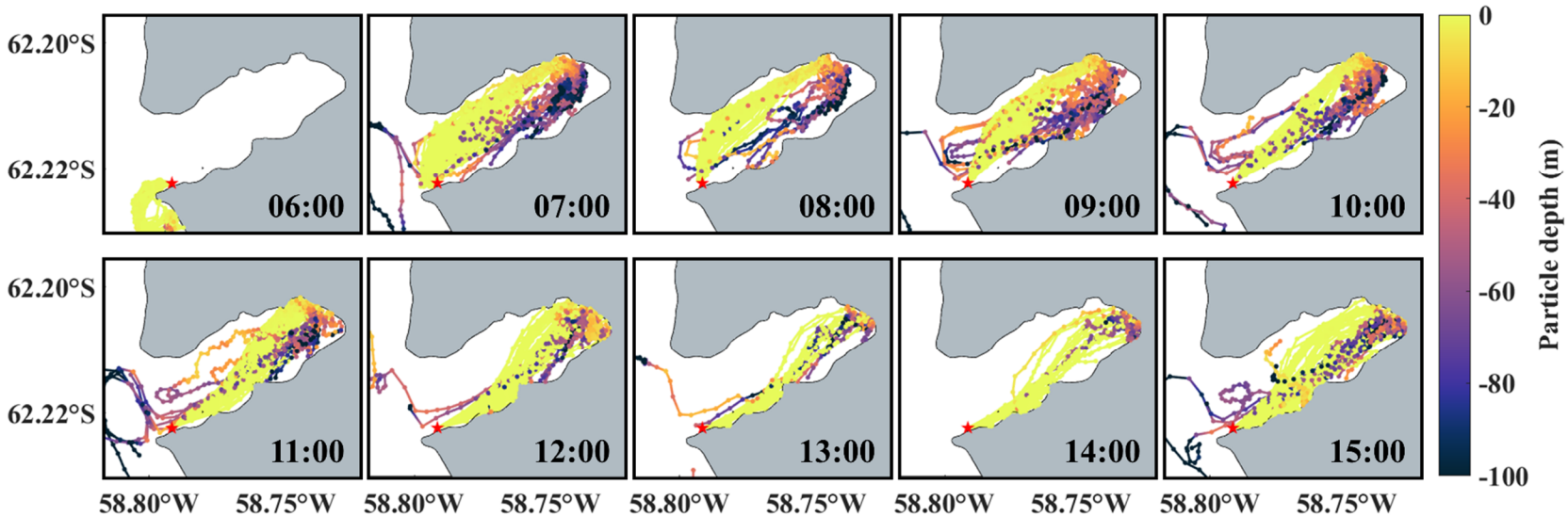

Figure 4.8 Trajectories of PP released at each time.

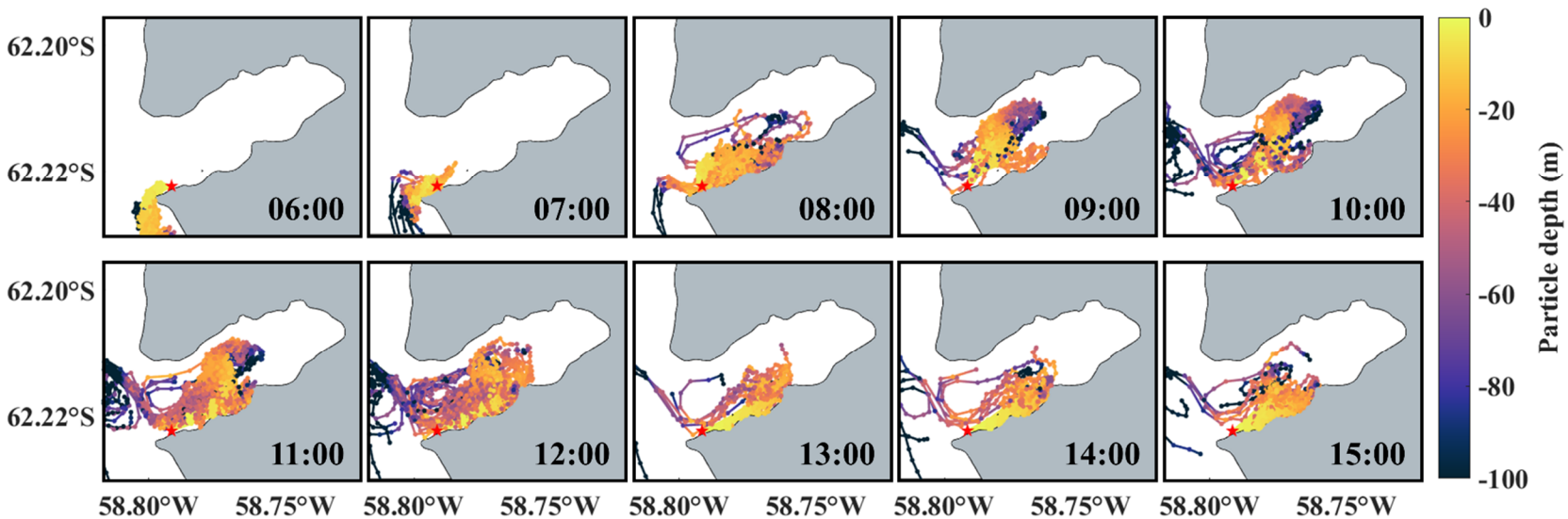

Figure 4.9 Trajectories of PET released at each time.

The particles' accumulation locations for each case were identified to where they were accumulated (Figure 4.10). All cases showed that most of PPs tended to land on the coast of the cove, while PETs were mostly accumulated to the seabed in the cove. Comparing the number of PP and PET, it was confirmed that more PP remained in Marian Cove than PET. This is because PP easily flowed into Marian Cove along the surface currents and landed on the coast in a short period. On the other hand, PETs relatively sank fast to the bottom layer, and so they could not easily enter Marian Cove and transport out to Maxwell Bay before accumulation. When particles were released at 06:00, which is the ebb time, all particles exited Marian Cove and reached near Barton Peninsula, separating Marian Cove and Potter Cove. On the other hand, at the flood time, most of the particles were easily introduced into Marian Cove along the current direction, and so they were landed or accumulated in Marian Cove. After 12:00, a substantial number of particles reached the southeast coast of Marian Cove due to the current direction at particle release time. Moreover, when the number of MPs remaining Marian Cove for each case is counted, significantly more MPs remain at the flood time compared to the ebb time (Figure 4.11). To sum up, discharging wastewater before the low tide can lower the MPs concentration in Marian Cove than discharging during the flood time.

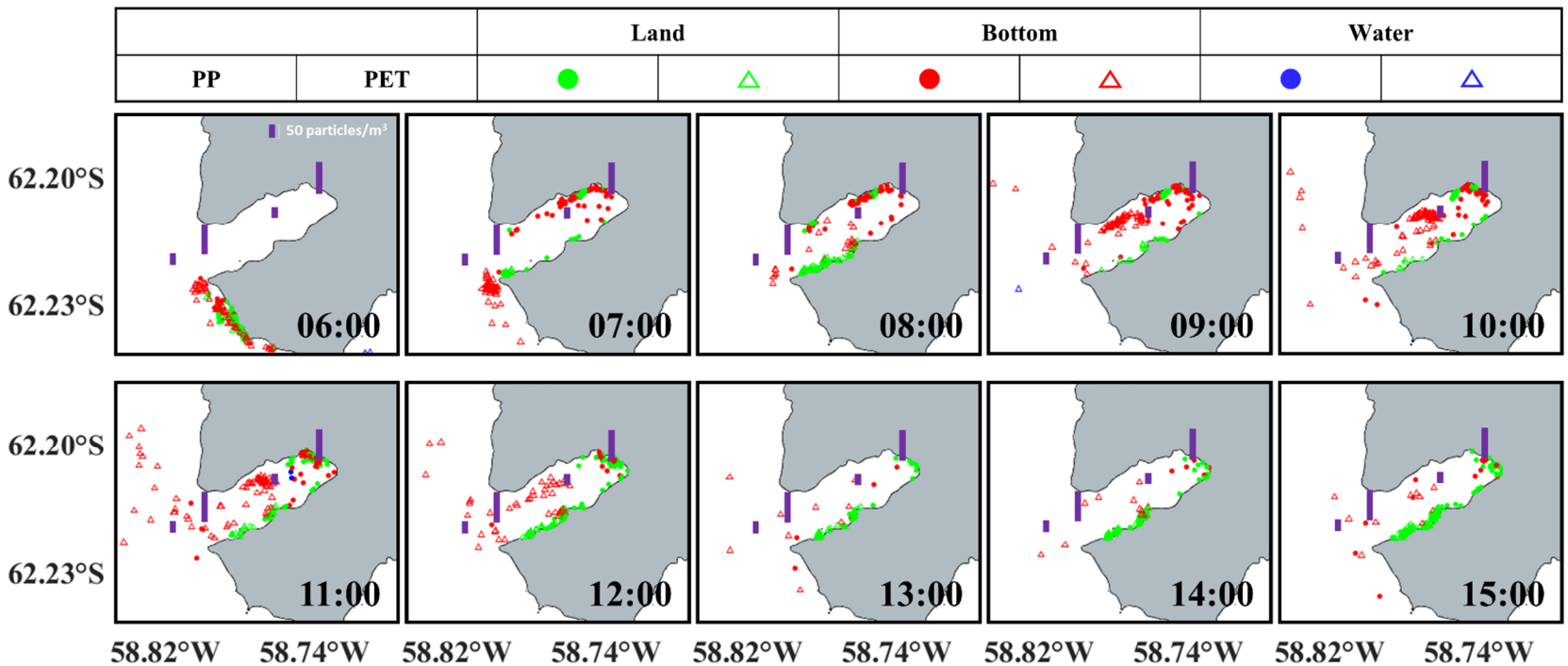

Figure 4.10 Particles' accumulation locations.

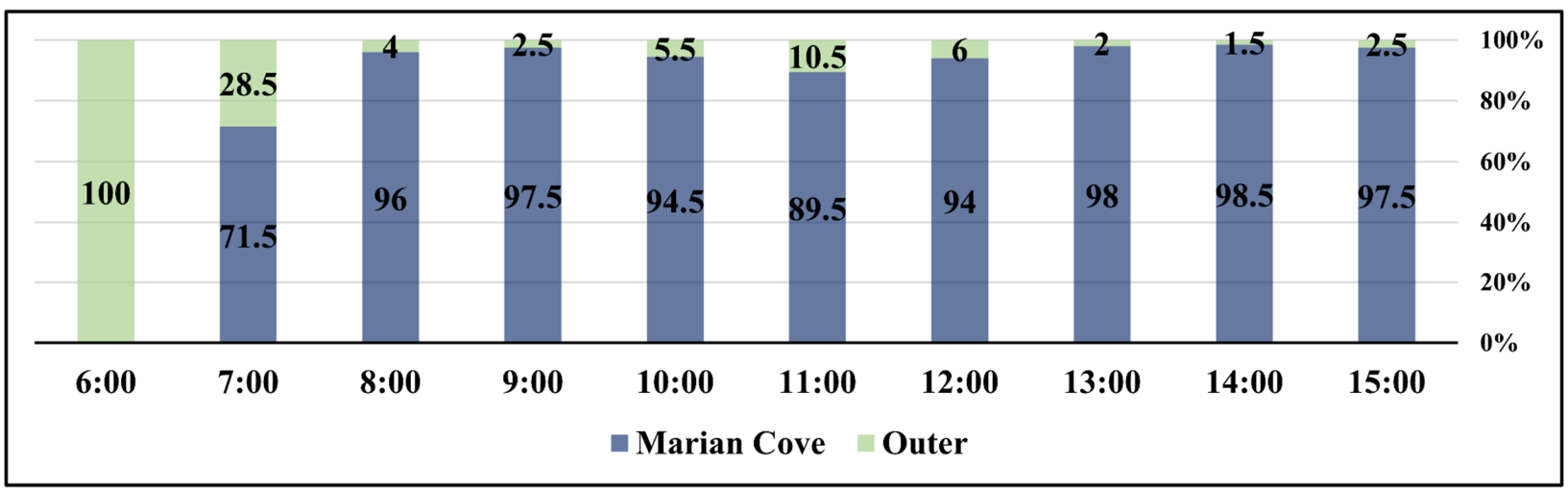

Figure 4.11 The remaining number of MPs.

4.4 MPs' trajectories depending on releasing location

Based on the trajectories of MPs depending on releasing time, the number of particles remaining Marian Cove can be reduced when the particles were released before the low tide, so it prevents them from accumulating in the cove. However, since the wastewater is discharged from the inside of the cove, direct contamination cannot be avoided in any way. Therefore, to reduce the accumulation of MPs inside the cove at all, two scenarios were constructed. One is to release particles from the shoreline near the King Sejong Station in the direction of Maxwell Bay, and the other is to release MPs from the surface water at a location inside the cove near the station. Both scenarios were simulated at 06:00 that is the ebb time, which may have the lowest MPs accumulation in Marian Cove.

In the first scenario, the particles were released from the entrance to Marian Cove (62.225°S, 58.798°W), bordering Maxwell Bay. As shown in Figure 4.12(a) and (b), they quickly sink to the bottom regardless of MPs' type. Particles sink fast along with the high downward velocity of seawater due to the rapid topographical changes. As mentioned in Section 4.2, compared to the HK angle, the vertical velocity of seawater dominates the MPs' vertical velocity in the vicinity of the particle release location. Therefore, since the particles' vertical velocity of the particle is not important, it can be said that both types of MPs are transported by the vertical velocity of seawater. The second simulation releases MPs from the surface of seawater a little far from the King Sejong Station (62.218°S, 58.798°W). In this case, all particles of both

polymers were transported to Maxwell Bay, and so no particle remains in Marian Cove (Figure 4.12(c) and (d)). PETs sink faster, but it was enough for them to exit Marian Cove. Furthermore, since particles were released away from the shoreline, most of the particles wandered around Maxwell Bay without reaching the shoreline after the release.

Consequentially, in the first scenario, MPs sink and may settle at the bottom due to the high vertical velocity of seawater caused by rapid topographical changes, but in the second scenario, all MPs can be transported to Maxwell Bay, regardless of the type of MPs. It means that the present location of the wastewater outlet of the King Sejong Station seems to be better than the first scenario's location in terms of preventing MPs from accumulating directly on the bottom. However, if the wastewater is discharged far from the coast using a pipeline, the concentration of MPs pollution in Marian Cove can be reduced. Accordingly, it is necessary to improve the method of discharging the wastewater of the station.

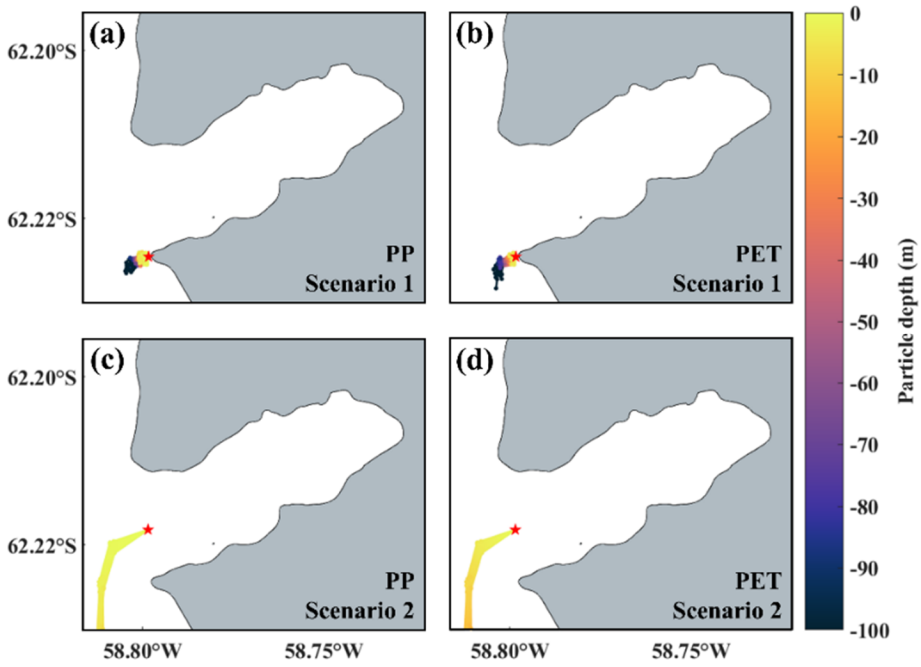

Figure 4.12 Trajectories of PP [(a), (c)] and PET [(b), (d)] released from two different locations: Scenario 1 [(a), (b)] and Scenario 2 [(c), (d)].

CHAPTER 5. SUMMARY AND SUGGESTION

This study elucidated the transport of MPs contained in the wastewater from the King Sejong Station. Although the King Sejong Station has a sewage treatment facility using the IC/SBR process, which is expected to have high removal efficiency of MPs, in actual, the efficiency of removing MPs from the sewage treatment plant of the station is remarkably low. So, many types of polymers were found without proper removal from the wastewater, and thus the dominant PP and PET were tracked in this work.

According to the HK angle that can determine the dominant force influencing the migrations of particles in the vertical direction, the buoyant particles, PPs, were mainly transported along the surface currents, and so they mostly reached the coast. The denser particles, PETs, sank to the lower layer fast due to their falling velocity, and so they were mainly accumulated to the seabed. PP floating around the surface layer can be transported in a short period compared to PET because the surface current is faster than lower layers. Moreover, in the flood, waves make PP and PET travel longer by 75% and 45%, respectively, and the migration speed of MPs is twice faster than the calm weather. In addition, the number of PETs remaining in Marian Cove increased when considering waves, which means that waves can change the direction of the flow, and so it is a major factor to track the MPs' trajectories.

The releasing time related to the tidal cycle also determined the

accumulation and concentration of MPs in Marian Cove. Both PPs and PETs released at 06:00 that is the ebb were not transported into Marian Cove but out to Maxwell Bay, and those released in the flood traveled into Marian Cove and circulated inside. PPs released at 08:00 that is the low tide followed the flood currents, and all particles remained in Marian Cove. In the case of PETs, they were not transported away from the releasing location and floated near the entrance of the cove, so they have a little chance of transporting out to Maxwell Bay. According to the MPs' accumulation locations, most of PPs tended to land on the coast in a short period, while PETs were accumulated to the seabed. Also, it is indicated that discharging the wastewater before the low tide can reduce the remaining number of MPs in Marian Cove.

However, there is one problem here: all the particles released at 06:00 reached the shoreline of Barton Peninsula, where the penguin village designated as an Antarctic Specially Protected Area (ASPA) is located. Although the release of wastewater in the ebb can reduce the accumulations of MPs pollution in Marian cove, discharge from the current location of the station can affect the environmental soundness of ASPA. Accordingly, consideration of releasing location is required since when the particles were released from seawater a little far from the coast in the ebb, all particles floated out to Maxwell Bay unhindered by the shoreline. The present study suggests that the wastewater discharged from the scientific research station located inside the cove can play a role as an important source of MPs pollution on a local scale, and so the best way to discharge the wastewater is to release it from seawater a

little off the coast before the low tide.

In the Protocol on Environmental Protection to the Antarctic Treaty, there are two Annexes related to discharge wastewater from the station and vessels: Waste Disposal and Waste Management (Annex III) and Prevention of Marine Pollution (Annex IV) (Antarctic Treaty Secretariat, 1998a, 1998b). Annex IV stipulates that all untreated discharges from the vessels should be eliminated within 12 nautical miles of land or ice shelf. However, the wastewater from the scientific research station is not regulated to be treated in a more rigorous method than the maceration method in Annex III. Moreover, the Protocol does not contain any restrictions on the treatment of MPs contained in the wastewater. Reed et al. (2018) stated that studies on MPs pollution within Antarctica, especially around the scientific research stations, were not sufficiently conducted, so the Antarctic Treaty Consultative Parties had not held a comprehensive discussion of MPs. But now, based on many studies, it is clear that MPs pollution within Antarctica is becoming serious. Therefore, to mitigate MPs contamination of the Antarctic Ocean, it is recommended that the criteria for discharging wastewater be subdivided to cover MPs treatment.

REFERENCES

Carter, L., McCave, I., Williams, M.J., 2008. Circulation and water masses of the Southern Ocean: a review. Developments in earth and environmental sciences 8, 85-114.

Chaparro, M.A., Nuñez, H., Lirio, J.M., Gogorza, C.S., Sinito, A.M., 2007. Magnetic screening and heavy metal pollution studies in soils from Marambio station, Antarctica. Antarctic Science 19, 379.

Chubarenko, I., Bagaev, A., Zobkov, M., Esiukova, E., 2016. On some physical and dynamical properties of microplastic particles in marine environment. Marine pollution bulletin 108, 105-112.

Cincinelli, A., Scopetani, C., Chelazzi, D., Lombardini, E., Martellini, T., Katsoyiannis, A., Fossi, M.C., Corsolini, S., 2017. Microplastic in the surface waters of the Ross Sea (Antarctica): occurrence, distribution and characterization by FTIR. Chemosphere 175, 391-400.

Curtosi, A., Pelletier, E., Vodopivez, C., St Louis, R., Mac Cormack, W.P., 2010. Presence and distribution of persistent toxic substances in sediments and marine organisms of Potter Cove, Antarctica. Archives of environmental contamination and toxicology 59, 582-592.

Deltares, 2017a. Delft3D-FLOW User Manual. Deltares Delft, The Netherlands.

Deltares, 2017b. Delft3D-WAVE User Manual. Deltares Delft, The Netherlands.

Dingemans, M., Radder, A., De Vriend, H., 1987. Computation of the driving forces of wave-induced currents. Coastal Engineering 11, 539-563.

Fraser, C.I., Morrison, A.K., Hogg, A.M., Macaya, E.C., van Sebille, E., Ryan, P.G., Padovan, A., Jack, C., Valdivia, N., Waters, J.M., 2018. Antarctica's ecological isolation will be broken by storm-driven dispersal and warming. Nature climate change 8, 704-708.

Gröndahl, F., Sidenmark, J., Thomsen1, A., 2009. Survey of waste water disposal practices at Antarctic research stations. Polar Research 28, 298-306.

Hidalgo-Ruz, V., Gutow, L., Thompson, R.C., Thiel, M., 2012. Microplastics in the marine environment: a review of the methods used for identification and quantification. Environmental science & technology 46, 3060-3075.

Isobe, A., Kubo, K., Tamura, Y., Nakashima, E., Fujii, N., 2014. Selective transport of microplastics and mesoplastics by drifting in coastal waters. Marine pollution bulletin 89, 324-330.

Isobe, A., Uchiyama-Matsumoto, K., Uchida, K., Tokai, T., 2017. Microplastics in the southern ocean. Marine pollution bulletin 114, 623-626.

Iwasaki, S., Isobe, A., Kako, S.i., Uchida, K., Tokai, T., 2017. Fate of microplastics and mesoplastics carried by surface currents and wind waves: A numerical model approach in the Sea of Japan. Marine Pollution Bulletin 121, 85-96.

Jalón-Rojas, I., Wang, X.H., Fredj, E., 2019. A 3D numerical model to track marine plastic debris (TrackMPD): sensitivity of microplastic trajectories and fates to particle dynamical properties and physical processes. Marine pollution bulletin 141, 256-272.

Khatmullina, L., Isachenko, I., 2017. Settling velocity of microplastic particles of regular shapes. Marine pollution bulletin 114, 871-880.

Lee, H., Kim, Y., 2018. Treatment characteristics of microplastics at biological sewage treatment facilities in Korea. Marine pollution bulletin 137, 1-8.

Llanillo, P., Aiken, C.M., Cordero, R., Damiani, A., Sepúlveda, E., Fernández-Gómez, B., 2019. oceanographic Variability induced by tides, the intraseasonal cycle and Warm Subsurface Water intrusions in Maxwell Bay, King George island (West-Antarctica). Scientific reports 9, 1-17.

Mellor, G.L., Yamada, T., 1982. Development of a turbulence closure model for geophysical fluid problems. Reviews of Geophysics 20, 851-875.

Munari, C., Infantini, V., Scoponi, M., Rastelli, E., Corinaldesi, C., Mistri, M., 2017. Microplastics in the sediments of Terra Nova Bay (Ross Sea, Antarctica). Marine pollution bulletin 122, 161-165.

Pawlowicz, R., Beardsley, B., Lentz, S., 2002. Classical tidal harmonic analysis including error estimates in MATLAB using T_TIDE. Computers & Geosciences 28, 929-937.

PlasticsEurope, 2020. Plastics–the Facts 2019, Information accessed at

http://www.-plasticseurope. org/application. 2020, PlasticsEurope.

Pugh, D.T., 1987. Tides, surges and mean sea level.

Reed, S., Clark, M., Thompson, R., Hughes, K.A., 2018. Microplastics in marine sediments near Rothera research station, Antarctica. Marine pollution bulletin 133, 460-463.

Waller, C.L., Griffiths, H.J., Waluda, C.M., Thorpe, S.E., Loaiza, I., Moreno, B., Pacherres, C.O., Hughes, K.A., 2017. Microplastics in the Antarctic marine system: an emerging area of research. Science of the Total Environment 598, 220-227.

Yoo, K.-C., Lee, M.K., Yoon, H.I., Lee, Y.I., Kang, C.Y., 2015. Hydrography of Marian Cove, King George Island, West Antarctica: implications for ice-proximal sedimentation during summer. Antarctic Science 27, 185-196.

Yoo, K.-C., Yoon, H.I., Oh, J.-K., Kim, Y., Kang, C.Y., 1999. Water Column Properties and Dispersal Pattern of Suspended Particulate Matter (SPM) of Marian Cove during Austral Summer, King George Island, West Antarctica. Journal of the Korean Society of Oceanography 4, 266-274.

Zhiyao, S., Tingting, W., Fumin, X., Ruijie, L., 2008. A simple formula for predicting settling velocity of sediment particles. Water Science and Engineering 1, 37-43.

국문초록

서남극 마리안 소만에서의 미세플라스틱 이송

서울대학교 대학원

건설환경공학부

김 보 경

청정해역으로 알려진 남극해에서 발견된 5 mm 이하 크기의 미세플라스틱의 기원은 크게 남극해 외부와 내부 두 가지로 추정된다. 한 조사에 따르면, 남극에 상주하는 연구 과학 기지의 반 이상이 적절한 하수처리 시스템을 갖추고 있지 않기 때문에 기지의 방류수가 남극해에 지역적인 영향을 미치는 원인으로 추측될 수 있다. 현장 조사를 통해 남극 세종과학기지가 위치한 만에서 미세플라스틱이 집적되고 있음을 확인하였고, 방류수에서 발견된 미세플라스틱의 농도가 주변 해수에 비해 약 1000배 이상 높은 것으로 보아, 방류수에 포함된 미세플라스틱이 기지 주변 해수 오염의 주요 원인으로 예상된다.

본 연구에서는 만 내에서의 미세플라스틱 이동 및 집적 메커니즘을 조사하기 위해 수치 모델을 통해 세종과학기지 주변장의 흐름을 재현하고, 미세플라스틱의 특성을 반영한 Lagrangian Particle Tracking 방법을 이용해 입자의 궤적을 파랑 효과, 방출 시간, 방출 위치에 따라 추적하였다. 수치 모의 결과, 세종과학기지가 위치

한 마리안 소만은 멕스웰 만에 비해 유속이 느리며, 파랑의 효과를 고려하면 표층 흐름에 상당한 영향을 미치므로 표층을 부유하는 입자의 움직임에 영향을 미칠 수 있다. 해수의 밀도보다 가벼운 입자들은 표층을 부유하며 더 오래 이동할 수 있기 때문에 대부분 해안선에 도달할 수 있었고, 무거운 입자들은 상대적으로 빠른 속도로 가라 앉으며 해저에 집적되었다. 또한, 파랑의 효과를 고려하면 입자의 이동 속도를 두 배로 증가시켰다. 이는 파랑과 같은 물리해양학적인 프로세스가 표층을 부유하는 입자의 이송에 중요한 요소임을 의미한다.

또한, 미세플라스틱이 심각한 환경 및 생태계 문제를 야기할 수 있는 곳에 집적되는 것을 줄이기 위한 방법을 제안했다. 마리안 소만 내부의 미세플라스틱 농도를 줄이기 위해서는 간조 전 방류수를 방출하는 것이 가장 효과적이나, 입자들이 남극특별보호구역 근처에 집적됨을 보였다. 해안선에서 떨어진 해수에서 간조 전에 입자를 방출하게 된다면, 모든 입자들이 방출 직후 해안가에 도달하지 않고 마리안 소만을 빠져나가 외해로 이송됨을 보였다. 따라서, 기지에서 방출되는 방류수에 포함된 미세플라스틱의 집적량 결정에 있어 조석 주기에 따라 방류수를 방출해야 하는 장소와 시기를 제어하는 방법이 매우 중요하다.

주요어: 미세플라스틱, 파랑, 조석, 남극해, 남극 과학 기지, 방류수

학번: 2019-24281